doi:10.1038/nature11208

SUPPLEMENTARY INFORMATION

Autistic-like social behaviour in *Shank2*-mutant mice improved by restoring NMDA receptor function

Hyejung Won[1,2]*, Hye-Ryeon Lee[3]*, Heon Yung Gee[4]*, Won Mah[1,2]*, Jae-Ick Kim[3]*, Jiseok Lee[1,2], Seungmin Ha[1,2], Changwook Chung[1,2], Eun Suk Jung[4], Yi Sul Cho[5], Sae-Geun Park[1], Jung-Soo Lee[4], Kyungmin Lee[6], Daesoo Kim[1], Yong Chul Bae[5], Bong-Kiun Kaang[3,7], Min Goo Lee[4] & Eunjoon Kim[1,2,8,9]

[1]Department of Biological Sciences, KAIST, Daejeon 305-701, Korea; [2]National Creative Research Initiative Center for Synaptogenesis, KAIST, Daejeon 305-701, Korea; [3]National Creative Research Initiative Center for Memory, Department of Biological Sciences, College of Natural Sciences, Seoul National University, Gwanangno 599, Gwanak-gu, Seoul 151-747, Korea; [4]Department of Pharmacology, Brain Korea 21 Project for Medical Sciences, Severance Biomedical Science Institute, Yonsei University College of Medicine, Seoul 120-752, Korea; [5]Department of Oral Anatomy and Neurobiology, School of Dentistry, Kyungpook National University, Daegu 700-412, Korea; [6]Department of Anatomy, School of Medicine, Brain Science & Engineering Institute, Kyungpook National University, Daegu 700-412, Korea; [7]Department of Brain and Cognitive Sciences, Seoul National University, Seoul 151-747, Korea; [8]Graduate School of Nanoscience and Technology (World Class University), KAIST, Daejeon 305-701, Korea; [9]Center for Synaptic Brain Dysfunctions, Institute for Basic Science, Daejeon 305-811, Korea. *These authors contributed equally to this work.

SUPPLEMENTARY FIGURE LEGENDS

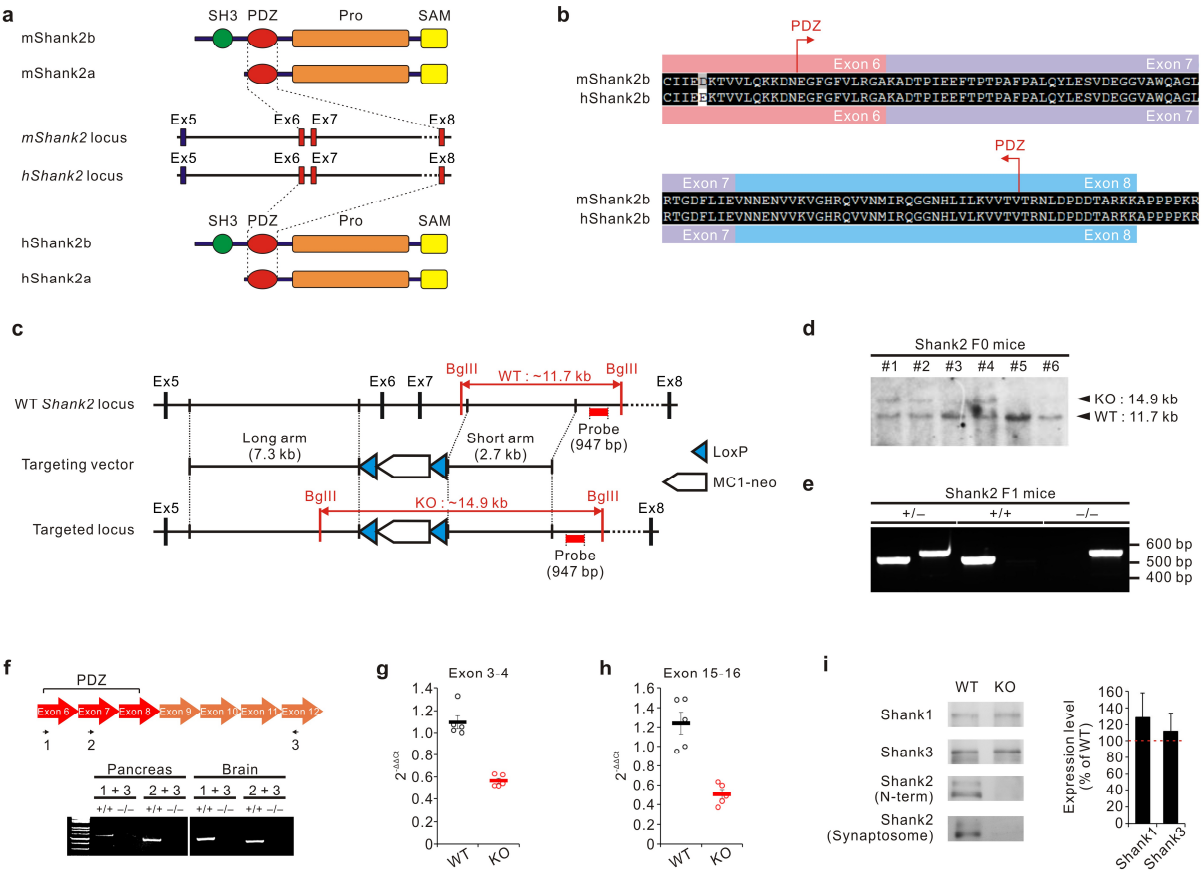

Supplementary Fig. 1. Identical exon-intron structures of mouse and human *Shnak2* genes in the region of the PDZ domain, and characterization of *Shank2* expression in *Shank2*$^{-/-}$ mice by Southern blot, PCR, RT-PCR, real-time PCR, and immunoblot analyses.

(a) Deletion of exons 6/7 in the *Shank2* gene in *Shank2*$^{-/-}$ mice exactly mimics the microdeletion of exons 6 and 7 in the human *SHANK2* gene identified in ASD. In order to mimic the ASD-associated microdeletion in the human *SHANK2* gene, the targeting construct was designed to delete exons 6 and 7 of the mouse *Shank2* gene that encodes a large portion of the PDZ domain in both splice variants of Shank2 (Shank2a and Shank2b; NM_001081370 and NM_001113373, NCBI database), which correspond to ProSAP/CortBP1and ProSAP1A, respectively, in rats. Note that the PDZ and following domains are deleted by the frame shift. Exon numbers were assigned based on the cDNA sequence of Shank2b.

(b) Alignment of amino acid sequences of the PDZ domain regions from mouse and human Shank2b that are encoded by exons 6, 7, and 8.

(c) Location of the probes used for Southern blot analysis are indicated in the *Shank2* gene. Also indicated are the sizes of BglII-digested target Shank2 DNA fragments for wild-type and mutant alleles. Note that the targeting construct contains a 7.3 kb 5'-long arm and a 2.7 kb 3'-short arm fragments. Ex, exon.

(d) Verification of the *Shank2* mutant alleles by Southern blot analysis. Genomic DNAs from F0 mice tails were digested with *BglII* and hybridized with the probe to visualize wild-type (11.7 kb) and mutant (14.9 kb) Shank2 DNA fragments. Germ-line transmission of the mutant allele could be identified in three mouse lines (#1, #2, and #4).

(e) Genotypes of *Shank2*$^{-/-}$ mice were determined by PCR on tail DNAs of F1 mice.

(f) Reverse-transcription (RT)-PCR indicates that mRNAs containing *Shank2* exons 6 and 7 are not produced in the *Shank2*$^{-/-}$ brain and pancreas tissues of *Shank2*$^{-/-}$ mice. Locations of PCR primers are presented in the

upper-hand panel and their individual sequences are provided in Supplementary methods. Exon numbers are based on Shank2b (NM_001113373).

(g and h) Real-time PCR quantification indicates levels of two *Shank2* mRNA exons (exon 3–4 and exon 15–16) outside the truncated exons 6 and 7 are reduced in the *Shank2*$^{-/-}$ brain. The amount of mRNA in various regions is significantly reduced in *Shank2*$^{-/-}$ mice, indicating that these regions undergo nonsense-mediated mRNA decay. Two different Taqman probes recognize exons 3–4 (Mm01163746_mH) and exons 15–16 (Mm01163737_m1) of Shank2b. n = 5 (WT), 5 (KO); *** P< 0.001 by Student's t-test.

(i) Shank2 deletion does not cause compensatory increases in the levels of Shank1 and Shank3 in *Shank2*$^{-/-}$ brain, as determined by immunoblotting of whole brain homogenates (3–4 wks). Synaptosomes (2–3 months) were additionally used to test whether Shank2 proteins are absent in synaptic fractions. For synaptosomes, Shank2 antibody raised against the C-terminal SAM domain was used. Note that the N-term antibody (NeuroMab), which appears to recognize the N-terminal PDZ domain based on that the antibody was raised against the SH3 + PDZ region and recognizes both Shank2a and Shank2b sharing the PDZ domain region, did not detect the two bands, or other smaller bands (data not shown), suggesting that small N-terminal fragments of Shank2 are unlikely to be left over in *Shank2*$^{-/-}$ mice.

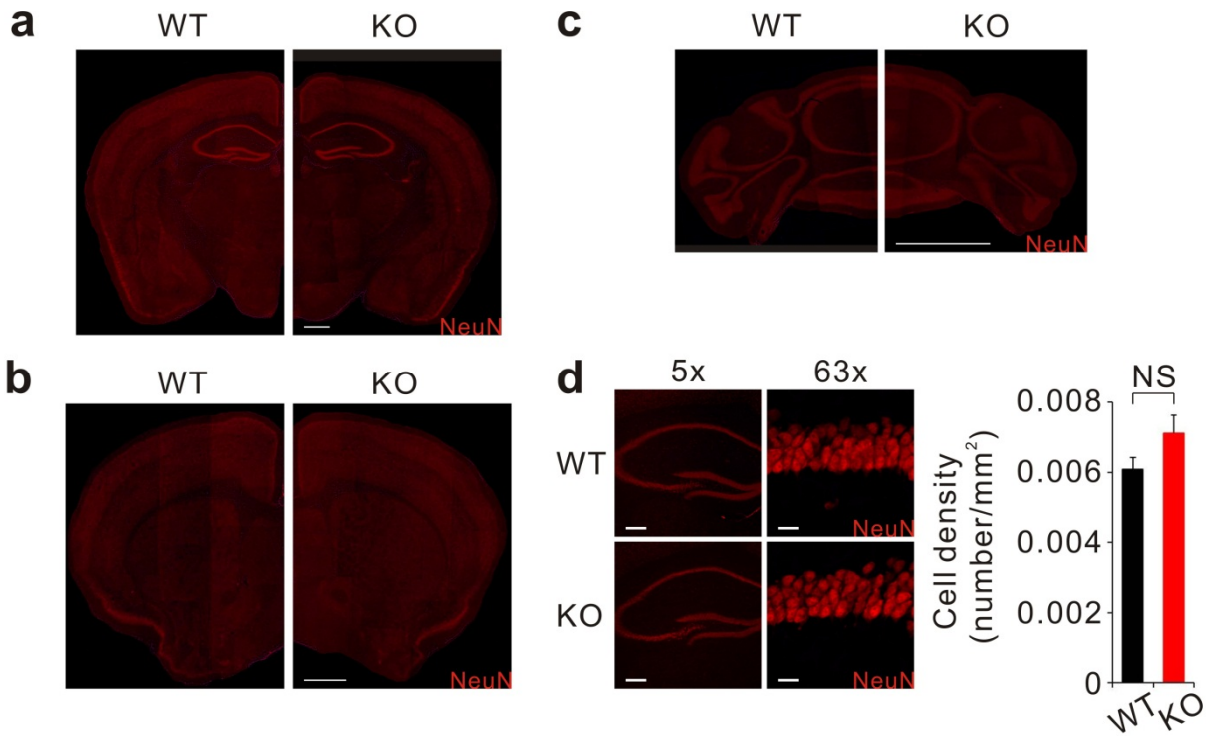

Supplementary Fig. 2. Normal gross morphology and neuronal cell number in the *Shank2*$^{-/-}$ brain.

Shank2$^{-/-}$ brain slices containing regions including the cortex (a), hippocampus (a), striatum (b), and cerebellum (c) were immunostained with antibodies against NeuN, a neuronal marker. (d) Quantification of neuronal cell numbers in the hippocampal formations of wild-type and *Shank2*$^{-/-}$ mice. Scale bars, 1.8 mm (a–c); 252 μm (d; 5x); 20 μm (d, 63x). n = 3 (WT), 3 (KO); NS, not significant; Student's t-test.

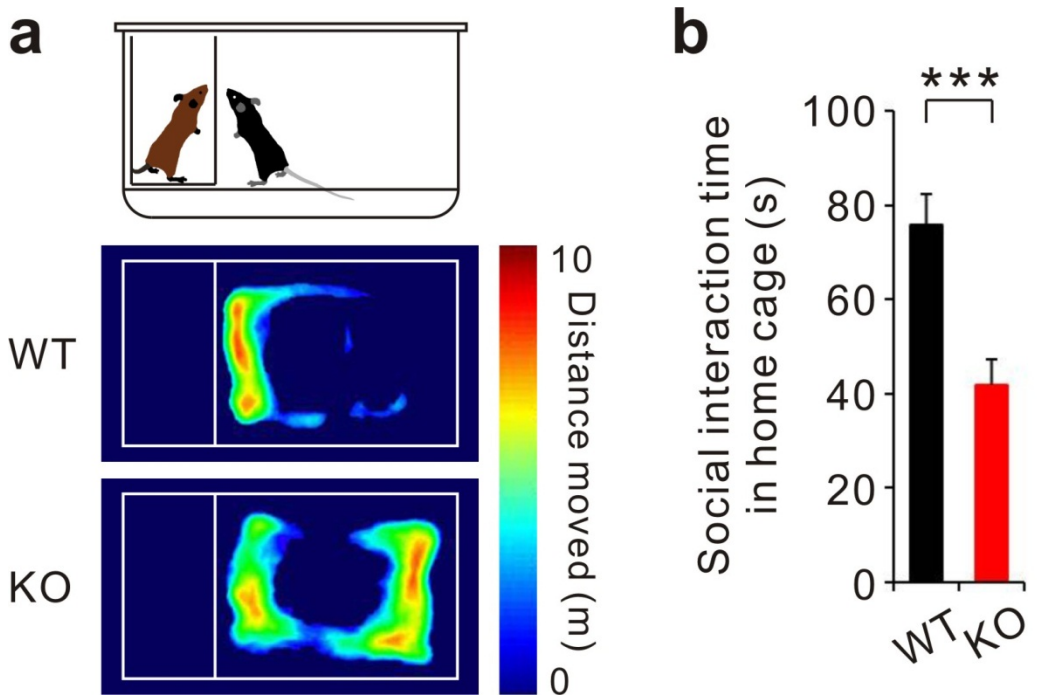

Supplementary Fig. 3. Impaired social interaction of *Shank2*$^{-/-}$ mice in home cages.

Wild-type or *Shank2*$^{-/-}$ (KO) male mice (black; 2–5 months) were allowed to explore a normal, male target mouse (brown; 2–4 months) separated by a transparent wall (a), followed by the analysis of time spent exploring the target mouse (b). The pseudo-colored heat map represents distance moved at each positions. n = 13 (WT), 14 (KO); ***P < 0.001, Student's t-test.

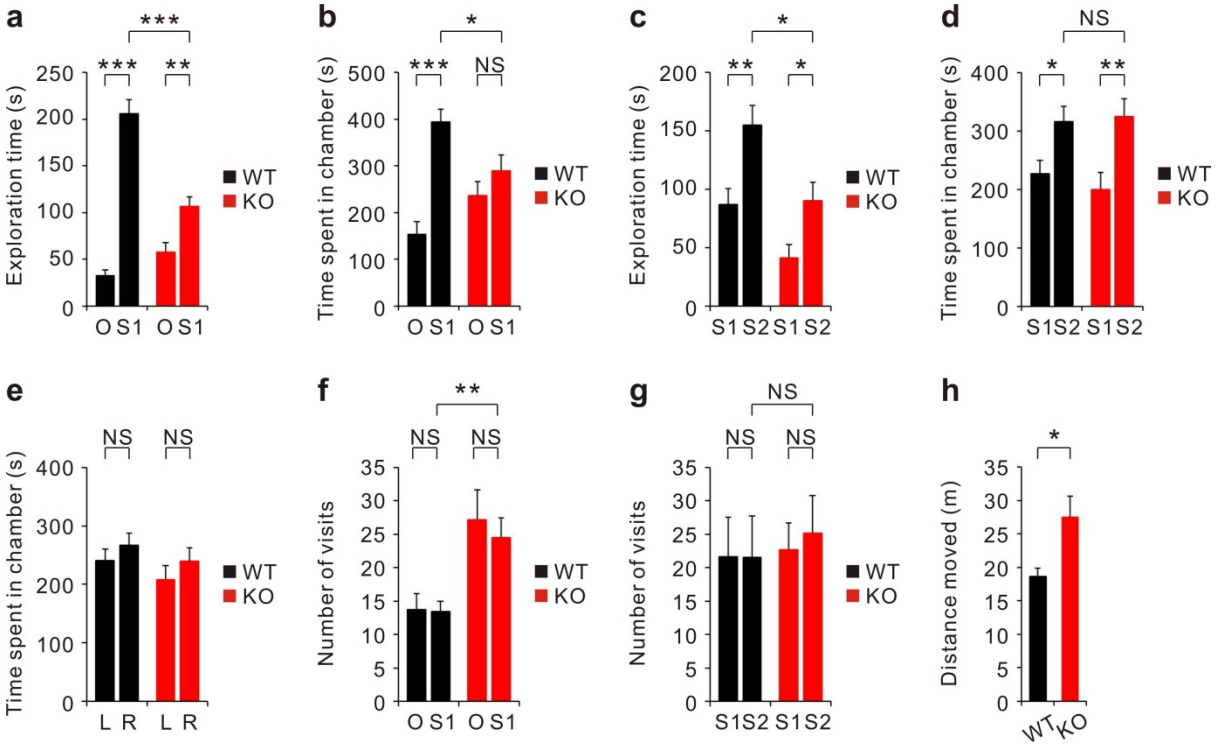

Supplementary Fig. 4. Reduced social interaction of *Shank2*$^{-/-}$ mice in three-chamber assays.

(a and b) *Shank2*$^{-/-}$ mice show reduced exploration of the target mouse (Stranger 1/S1) over the inanimate object (Object/O) relative to wild-type mice, as shown by exploration time (a) and time spent in chambers (b).

(c and d) *Shank2*$^{-/-}$ mice show comparable prefrence on the novel mouse (Stranger 2/S2) over the familiar mouse (S1) relative to wild-type mice, as shown by exploration time (c) and time spent in chambers (d).

(e) Wild-type and *Shank2*$^{-/-}$ mice equally explore the two opposite chambers (L/Left and R/Right) during the first 10-min habituation phase, suggesting that there is no pre-existing chamber bias.

(f–h) *Shank2*$^{-/-}$ mice show partial hyperactivity during three-chamber assays, as shown by the increased number of visits to both Object and Stranger 1 chambers relative to wild-type mice (f), although not in sessions for Stranger 1 and Stranger 2 (g), and also by the increased total distance moved during the exploration of the Object 1 or Stranger 1 (h). n = 11 (WT), 10 (KO); *P < 0.05, **P < 0.01, ***P < 0.001, NS, not significant; Student's t-test.

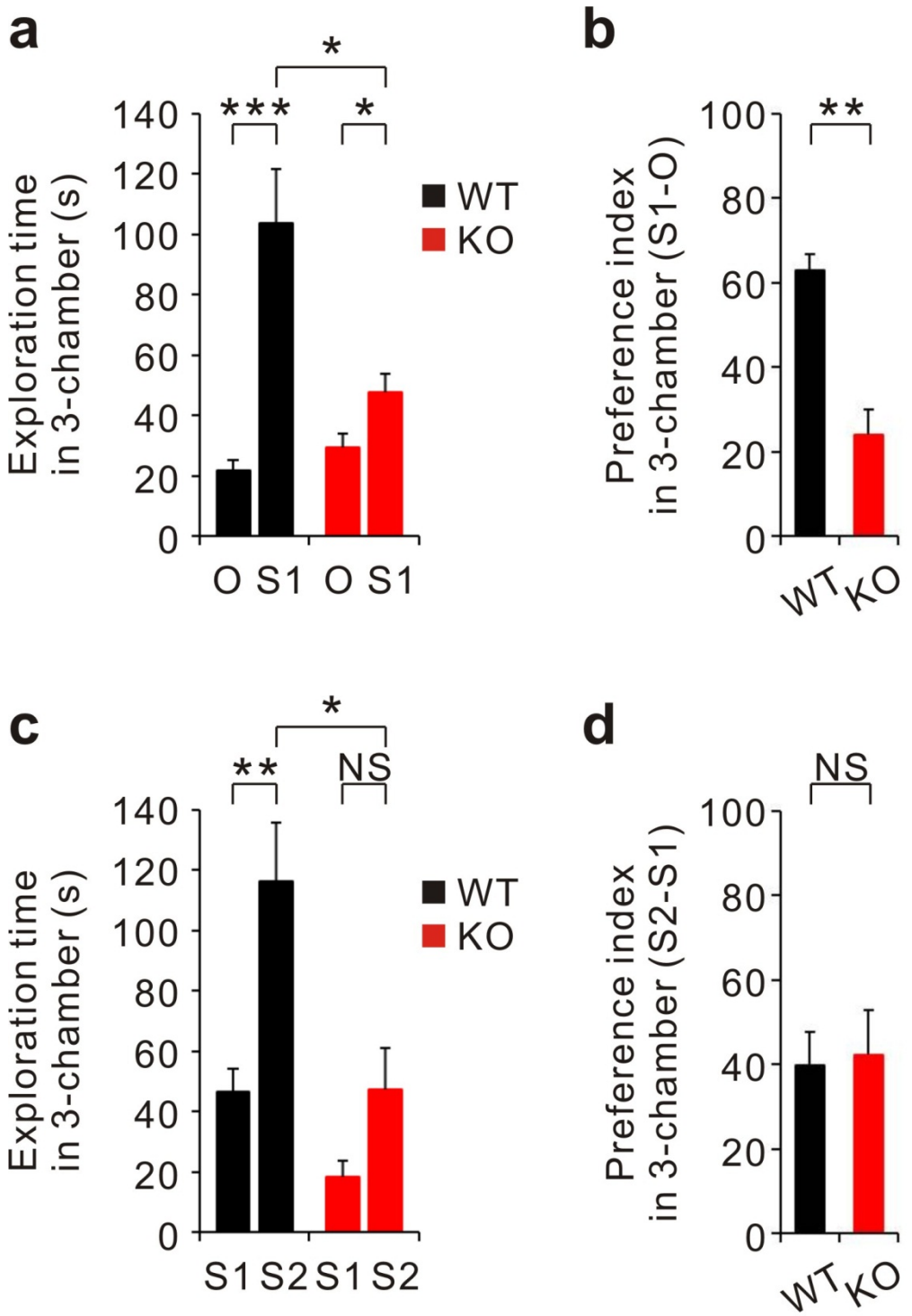

Supplementary Fig. 5. Juvenile *Shank2*$^{-/-}$ mice show impaired social interaction in three-chamber assays.

Juvenile wild-type or *Shank2*$^{-/-}$ mice (4–5 wks) were subjected to three-chamber social interaction assays. Note that *Shank2*$^{-/-}$ mice show reduced social interaction (a and b), but normal levels of social-novelty recognition (c and d). O, Object; S1, Stranger 1; S2, Stranger 2; n = 7 (WT), 5 (KO); *P < 0.05, **P < 0.01, ***P < 0.001, NS, not significant; Student's t-test.

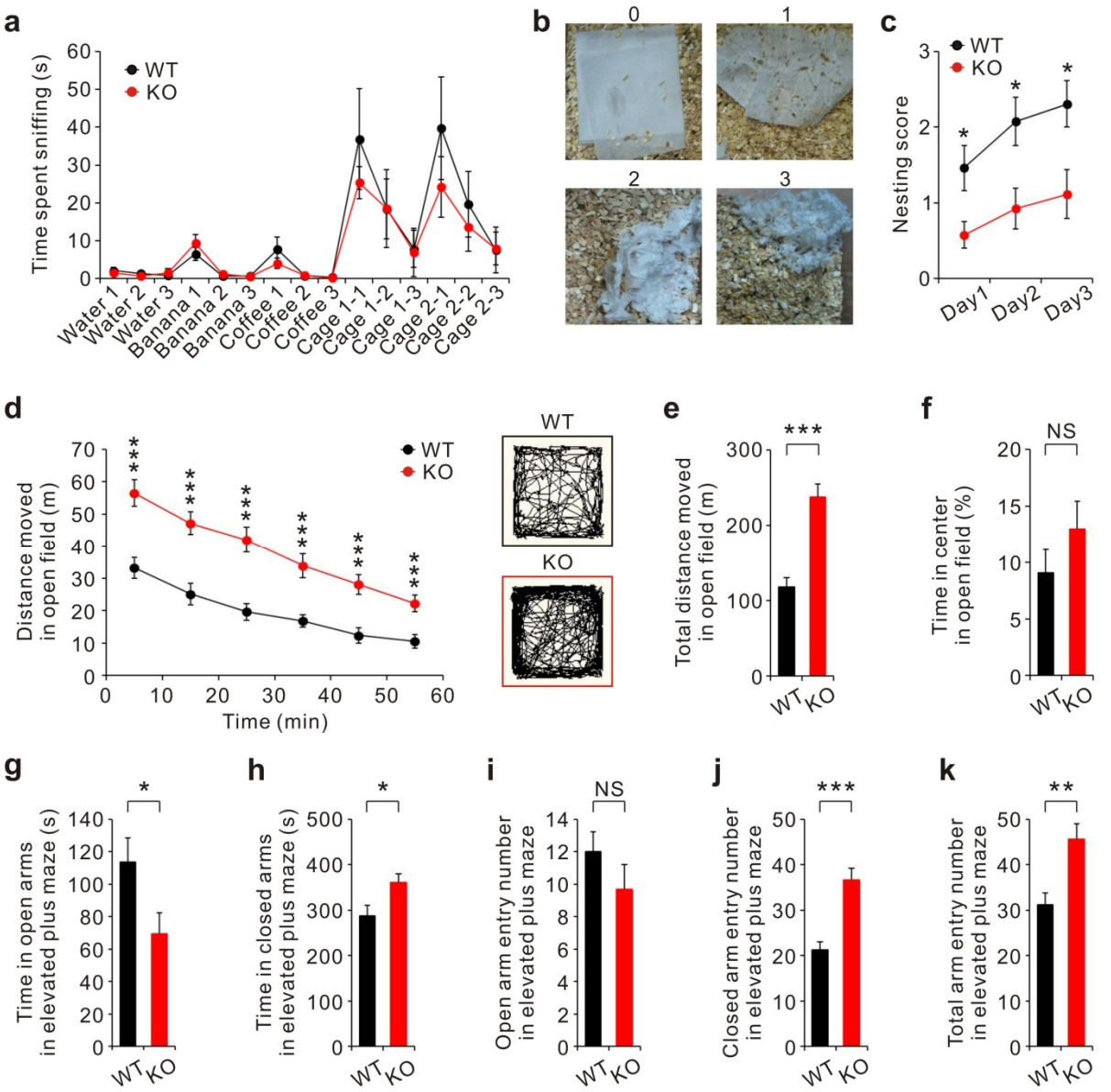

Supplementary Fig. 6. *Shank2*$^{-/-}$ mice show normal olfactory function, impaired nesting, hyperactivity, and anxiety-like behaviors.

(a) Normal olfactory function in *Shank2*$^{-/-}$ mice. Wild-type or *Shank2*$^{-/-}$ mice in their home cages were presented with a folded Kimwipes tissue soaked with water, non-social cues (banana, coffee) and social cues (cage 1 or 2 formerly occupied by another mouse) and monitored of their sniffing behaviors towards the target. n = 8 (WT), 7 (KO); Repeated measures ANOVA.

(b) Examples of nesting behaviors with increasing scores. Wild-type and *Shank2*$^{-/-}$ mice in their home cages were presented with sheets of tissue as a nest-building material and scored of nesting behaviors, by measuring the extent of converting the material into fine pieces over three days.

(c) Impaired nesting behavior in *Shank2*$^{-/-}$ mice. n = 13 (WT), 13 (KO); *$P < 0.05$; Student's t-test and repeated measures of ANOVA

(d–f) *Shank2*$^{-/-}$ mice show hyperactivity but normal anxiety-like behavior in an open field. Mice were allowed to explore an open field arena for 60 min, followed by quantification of the distance moved. *Shank2*$^{-/-}$ mice show hyperactivity in an open field arena, relative to wild-type mice (d and e), while they show comparable levels of locomotor activity in the center region of the open field, as shown by percent time spent in the center (f), indicative of normal levels of anxiety-like behavior in this assay. Examples of movement traces of wild-type

and *Shank2*$^{-/-}$ mice are shown in (d). NS, not significant. n = 13 (WT), 14 (KO); ***P < 0.001, NS, not significant; Student's t-test and repeated measure of ANOVA.

(g–k) *Shank2*$^{-/-}$ mice show anxiety-like behavior and hyperactivity in an elevated plus-maze. *Shank2*$^{-/-}$ mice show decreaesed time spent in open arms (g), increased time spent in closed arms (h) and increased number of closed, but not open, arm entries (i and j) relative to wild-type mice, indicative of anxiety-like behaviors in this assay. In addition, *Shank2*$^{-/-}$ mice show increased number of total arm entries (k), indicative of hyperactivity. n = 12 (WT), 12 (KO); *P < 0.05, **P < 0.01, ***P < 0.001, NS, not significant; Student's t-test.

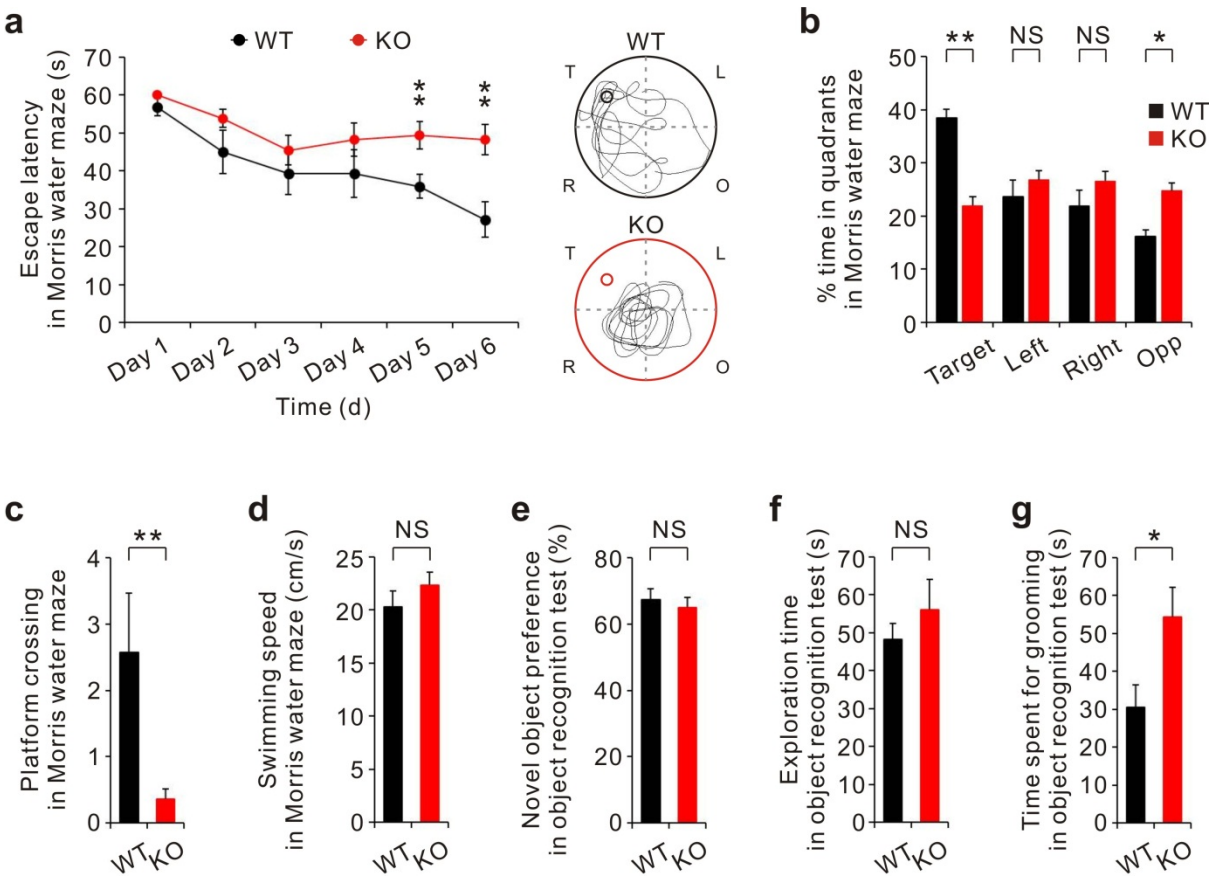

Supplementary Fig. 7. *Shank2*$^{-/-}$ mice show impaired spatial learning and memory in the Morris water maze, while they show normal novel object recognition.

(a–d) *Shank2*$^{-/-}$ mice perform poorly during the learning phase of the Morris water maze (a), spend reduced amount of time in the target quadrant during the probe test (b), less frequently cross the former platform area (c), and swim at normal speeds (d), relative to wild-type mice. T, Target; L, Left; R, Right; O, Opp; $n = 7$ (WT), 11 (KO); *$P < 0.05$, **$P < 0.01$, NS, not significant; Student's t-test and repeated measure of ANOVA.

(e) Normal levels of novel object recognition memory in *Shank2*$^{-/-}$ mice. Wild-type or *Shank2*$^{-/-}$ mice were allowed to explore two identical objects on the first day in an open field. Twenty-four hrs later, one of the two objects was replaced with a novel object, and the mice were allowed to explore the two objects.

(f) *Shank2*$^{-/-}$ mice spend comparable amounts of time exploring two identical objects relative to wild-type mice during the sample phase of novel object recognition tests.

(g) *Shank2*$^{-/-}$ mice spend more time in grooming behavior, relative to wild-type mice, during the sample phase of the novel object recognition test, indicative of ASD-like repetitive behavior. $n = 13$ (WT), 14 (KO); *$P <$ 0.05, NS, not significant; Student's t-test.

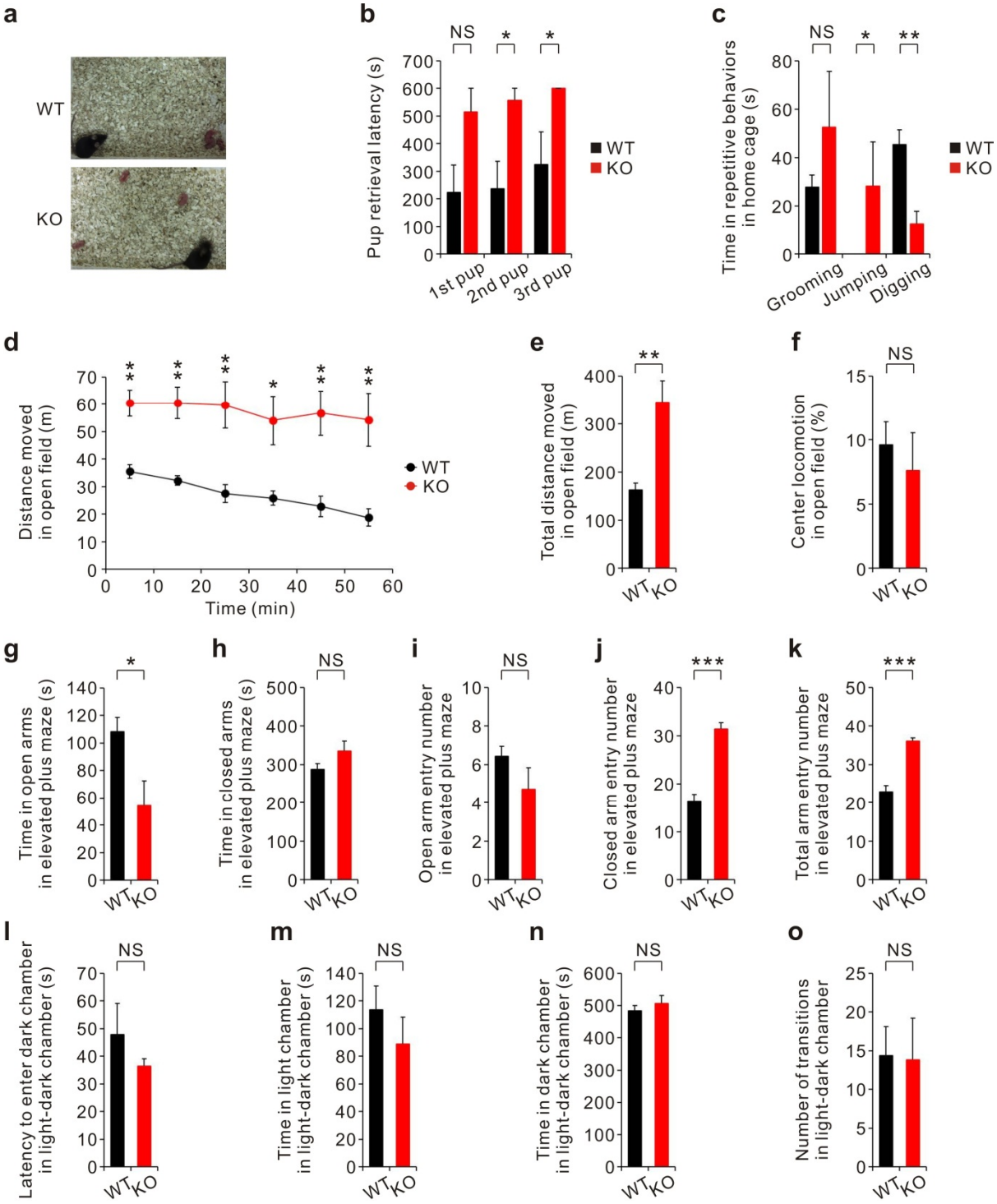

Supplementary Fig. 8. *Shank2*$^{-/-}$ female mice show impaired pup retrieval, hyperactivity in an open field, repetitive jumping, and anxiety-like behavior in an elevated plus-maze but not in a light-dark box.

(a and b) A wild-type or *Shank2*$^{-/-}$ virgin, female mouse was subjected to retrieve three pups that are scattered and isolated in a home cage (a; example images taken at the end of the session), followed by measurements of the time taken to retrieve the first, second, and third pups (b). $n = 5$ (WT), 5 (KO); $^{*}P < 0.05$; Student's t-test and repeated measure of ANOVA.

(c) Repetitive jumping, normal grooming, and reduced digging in *Shank2*$^{-/-}$ female mice. A mouse was placed in a stranger-free and fresh-bedded home cage and observed of the indicated repetitive behaviors. Note that jumping here represents jumping behavior significantly mixed with upright scrabbling, a form of repetitive

behavior related with wall-climbing stereotypy. n = 7 (WT), 7 (KO); *P < 0.05, **P < 0.01, NS, not significant; Mann-Whitney U test for jumping, Student's t-test for grooming and digging.

(d–f) Hyperactivity of *Shank2*$^{-/-}$ female mice in an open field assay. Mice were allowed to explore an open field arena for 60 min, followed by quantification of the distance moved (d and e) and time spent in the center region (f), a measure of anxiety-like behavior. n = 7 (WT), 7 (KO); *P < 0.05, **P < 0.01, NS, not significant; Student's t-test and repeated measure of ANOVA.

(g–k) *Shank2*$^{-/-}$ female mice show anxiety-like behaviors and hyperactivity in an elevated plus-maze. n = 14 (WT), 7 (KO); *P < 0.05, ***P < 0.001, NS, not significant; Student's t-test.

(l–o) *Shank2*$^{-/-}$ female mice show normal levels of anxiety-like behaviors comparable to wild-type animals in the light-dark box test, as shown by time spent for initial transition (l), time spent in light/dark chamber (m and n), and number of transitions (o). n = 11 (WT), 7 (KO); NS, not significant; Student's t-test.

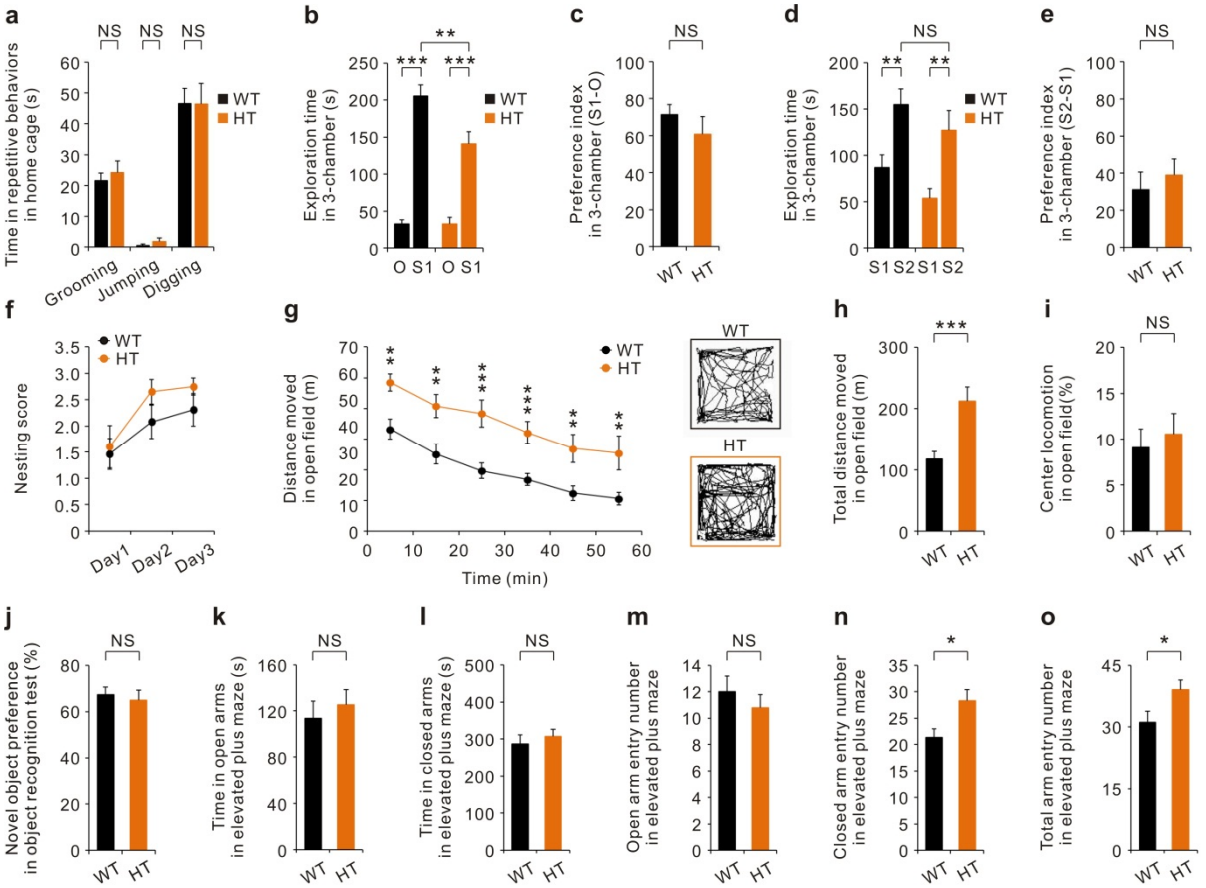

Supplementary Fig. 9. Heterozygous Shank2 (*Shank2*$^{+/-}$) mice show hyperactivity but normal repetitive behavior, social interaction, and anxiety-like behavior.

Shank2$^{+/-}$ mice show hyperactivity in an open field (g–i) and an elevated plus-maze (m–o), but no abnormalities in repetitive behaviors in home cages (a), 3-chamber social interaction (b–e), nesting behaviors (f), novel object recognition (j), and anxiety like-behaviors in an elevated plus-maze (k and l; normal time spent in open/closed arms). (a) n = 11 (WT/wild type), 6 (HT/hetero); (b–e) n = 11 (WT), 10 (HT); (f) n = 13 (WT), 9 (HT); (g-i) n = 13 (WT), 9 (HT); (k-o) n = 12 (WT), 10 (HT); O, Object; S1, Stranger 1; S2, Stranger 2; *$P < 0.05$, **$P < 0.01$, ***$P < 0.001$, NS, not significant; Student's t-test and repeated measures of ANOVA for nesting behavior (f) and open field (g).

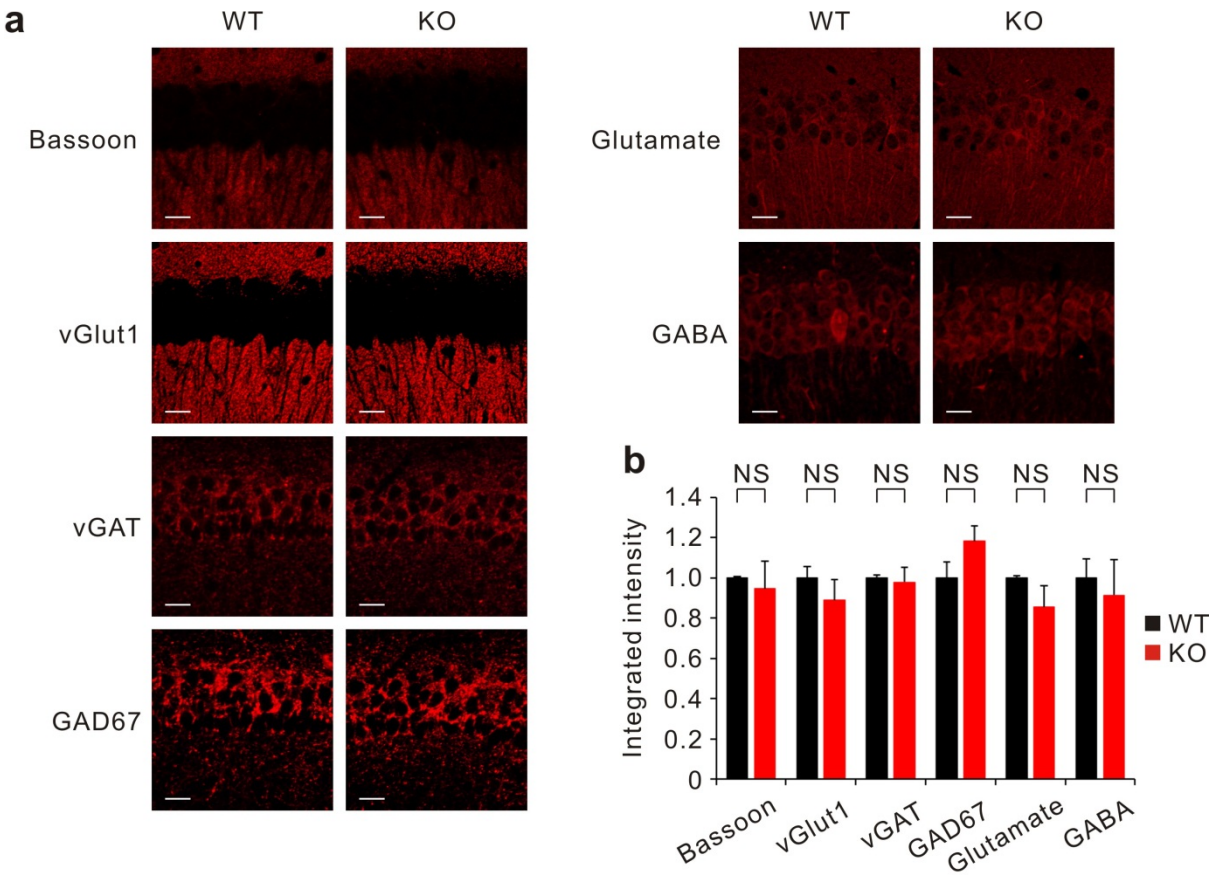

Supplementary Fig. 10. Normal synapse number in *Shank2*$^{-/-}$ mice determined by immunofluorescence staining.

Wild-type and *Shank2*$^{-/-}$ brain slices (3 months) were immunostained for synaptic marker proteins including bassoon (presynaptic), vGlut1 (excitatory presynaptic), vGAT (inhibitory presynaptic), GAD67 (inhibitory presynaptic), glutamate (excitatory neurotransmitter), and GABA (inhibitory neurotransmitter) (a; examples from the CA1 region of hippocampus), followed by quantification of the integrated intensities of the signals (b). Scale bars, 20 μm. n = 3 (WT), 3 (KO); NS, not significant; Student's t-test.

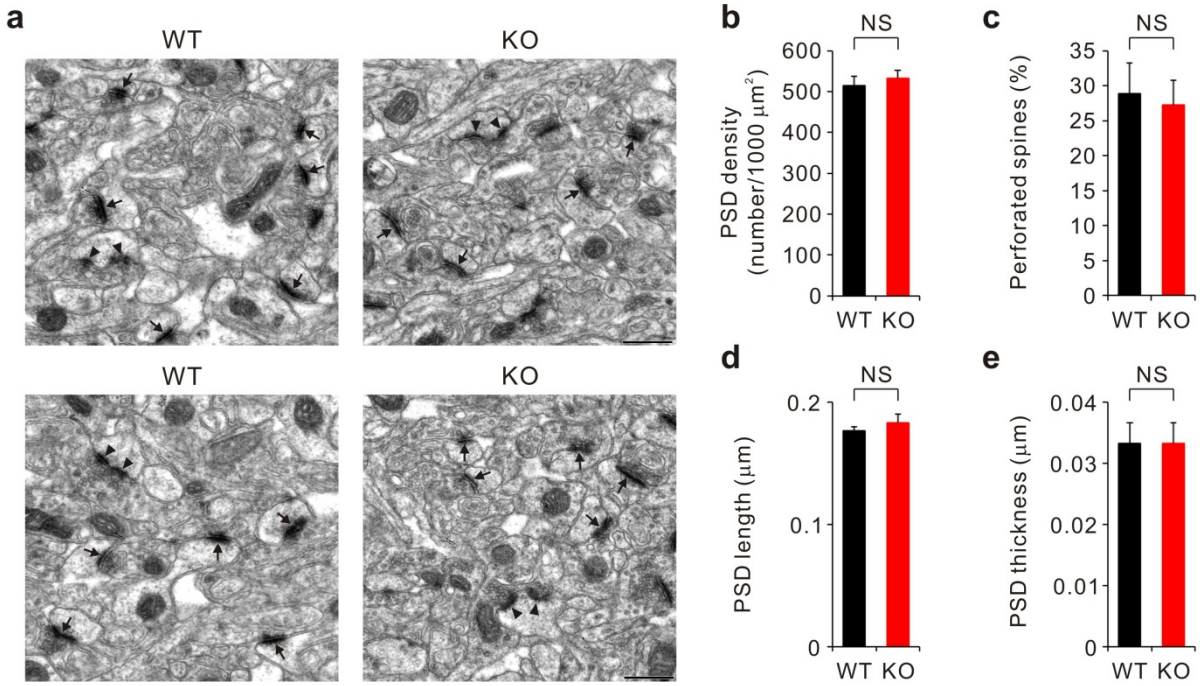

Supplementary Fig. 11. Normal excitatory synapse number and postsynaptic density morphology in *Shank2*$^{-/-}$ mice determined by electron microscopy.

Wild-type (WT) and *Shank2*$^{-/-}$ (KO) brain slices (8–9 wks) in the hippocampal CA1 region (stratum radiatum) were subjected to ultrastructural EM analysis. *Shank2*$^{-/-}$ mice show no alterations in the numbers of excitatory synapses, defined by active zones apposed to postsynaptic densities (PSDs; a and b; arrows), percentage of perforated spines (a and c; arrowheads), PSD length (d), and PSD thickness (e). n = 3 (WT), 3 (KO); NS, not significant; Student's t-test. Scale bar = 500 nm.

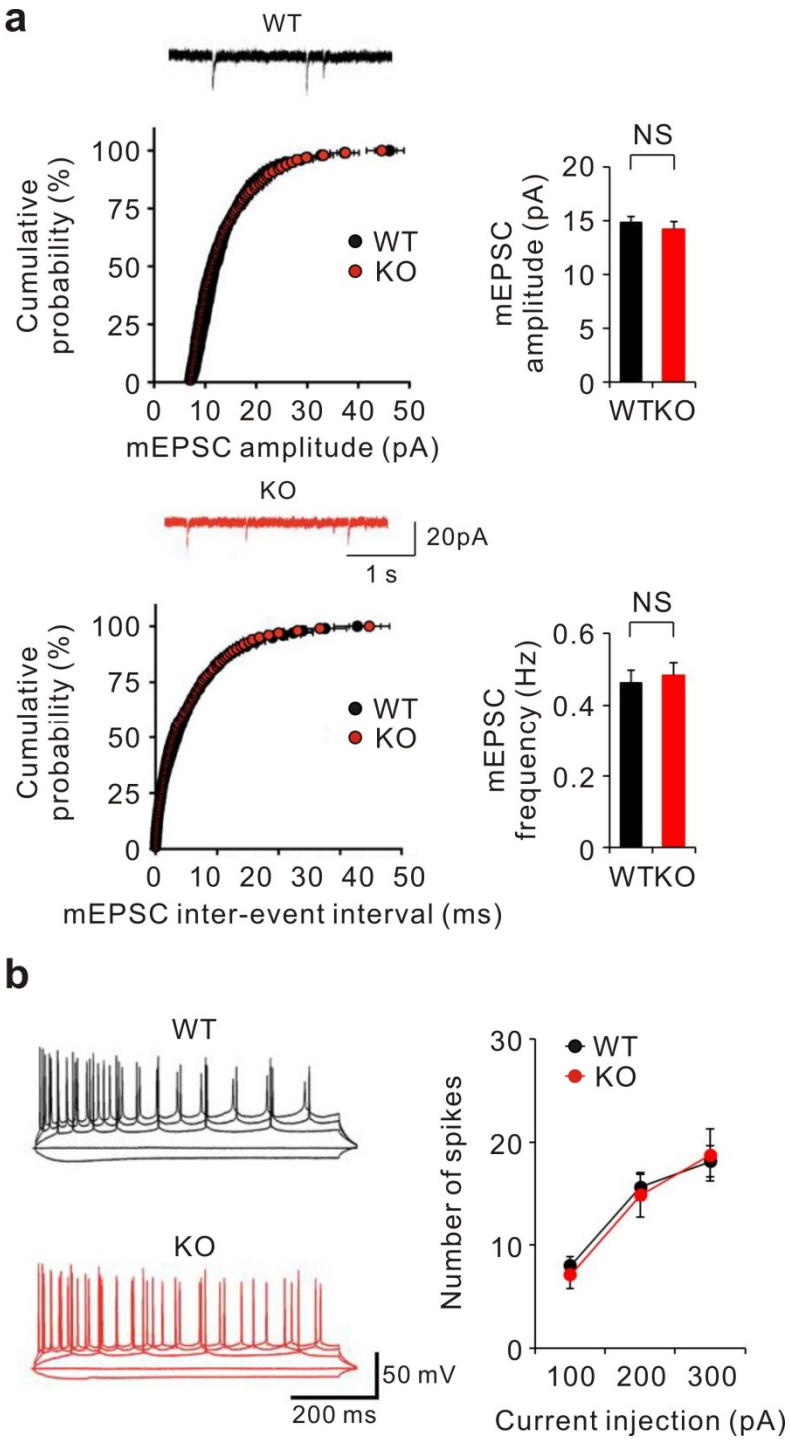

Supplementary Fig. 12. Normal miniature EPSCs and excitability in *Shank2*$^{-/-}$ CA1 pyramidal neurons.

(a) Normal amplitude and frequency of miniature EPSCs in *Shank2*$^{-/-}$ CA1 pyramidal neurons (amplitude, WT, 14.8 ± 0.6, 10 slices / 3 mice; KO, 14.2 ± 0.7, 10 slices / 3 mice; Student's t-test, NS, not significant; frequency, WT, 0.46 ± 0.04, 10 slices / 3 mice; KO, 0.48 ± 0.03, 10 slices / 3 mice; Student's t-test, NS, not significant).

(b) The number of spikes generated was similar between WT and *Shank2*$^{-/-}$ mice (100 pA, WT, 8.0 ± 0.9, KO, 7.1 ± 1.3, unpaired t-test, NS; 200 pA, WT, 15.6 ± 1.2, KO, 14.9 ± 2.2, Student's t-test, NS; 300 pA, WT, 18.1 ± 1.5, KO, 18.8 ± 2.6, Student's t-test, NS; WT, 8 slices / 2 mice, KO, 8 slices / 2 mice).

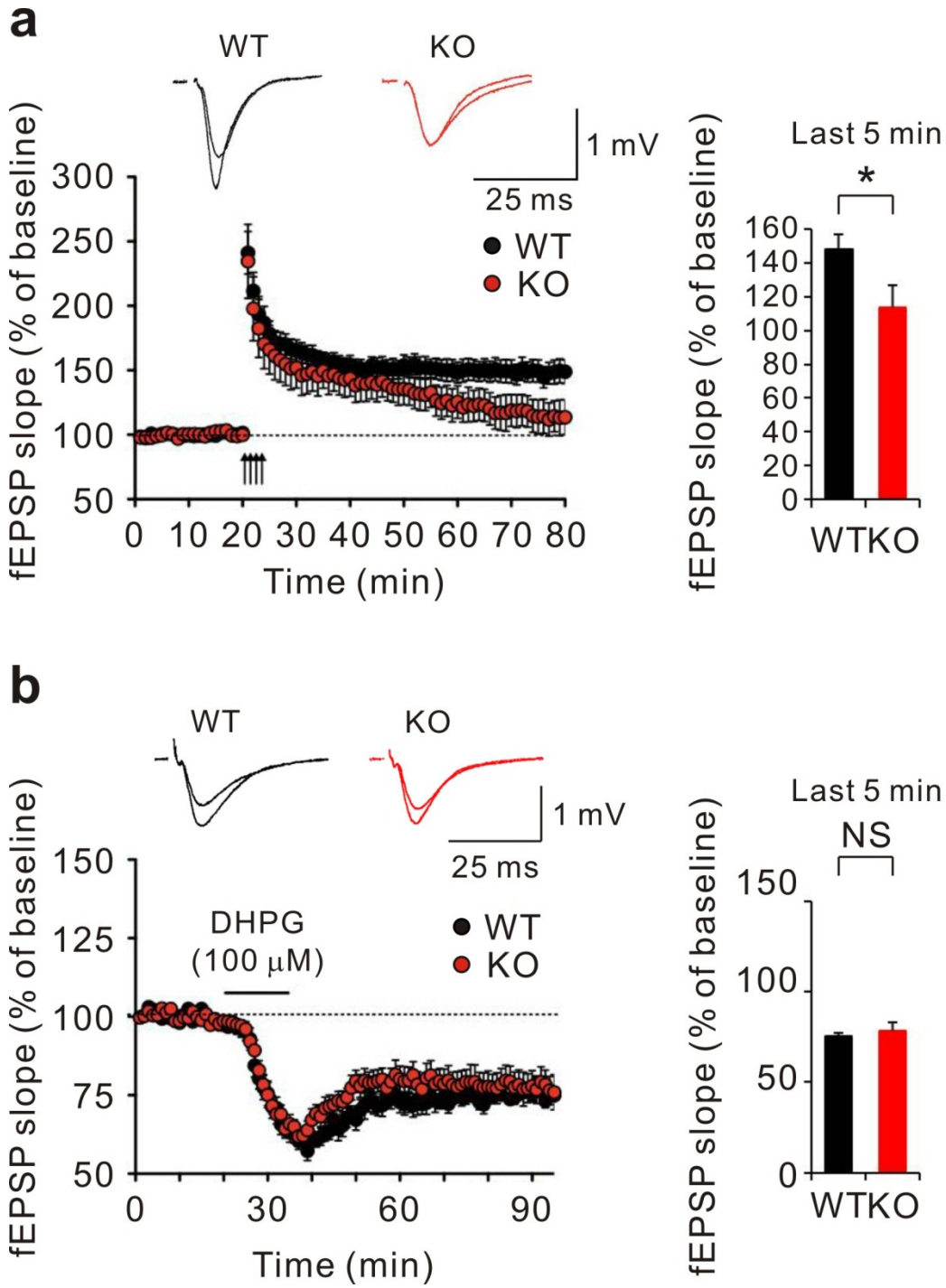

Supplementary Fig. 13. Impaired TBS-LTP and normal mGluR-LTD and at *Shank2*$^{-/-}$ SC-CA1 synapses.

(a) Impaired LTP induced by theta-burst stimulation (TBS) in *Shank2*$^{-/-}$ mice. Averages of fEPSP slopes at WT and *Shank2*$^{-/-}$ SC-CA1 synapses (left) during the last 5 min of the recording were compared (right) (WT, 147.9 ± 8.8, 9 slices / 4 mice; KO, 113.4 ± 13.1, 7 slices / 3 mice; Student's t-test, *P < 0.05).

(b) Normal mGluR-LTD induced by DHPG (mGluR5 agonist, 100 μM) at *Shank2*$^{-/-}$ SC-CA1 synapses. Averages of fEPSP slopes during the last 5 min of the recording were compared (right) (WT, 75.4 ± 1.8, 9 slices / 6 mice; KO, 78.6 ± 4.3, 8 slices / 6 mice; Student's t-test, NS, not significant).

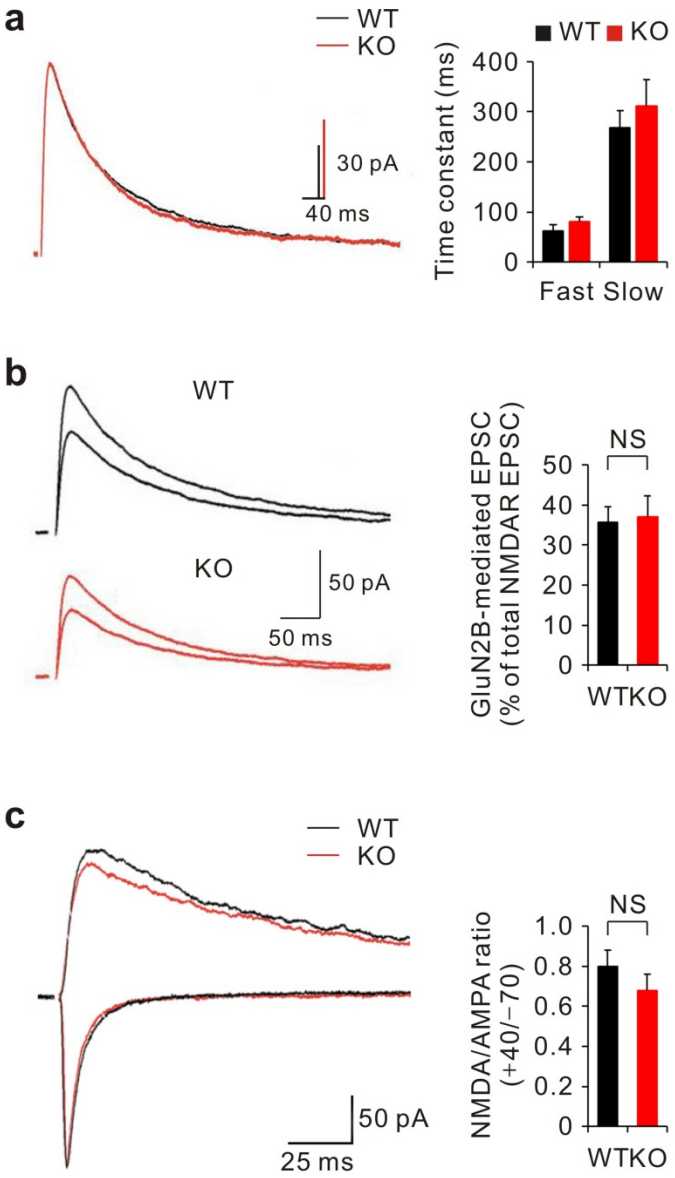

Supplementary Fig. 14. Normal decay kinetics and GluN2B-mediated currents in NMDAR EPSCs at *Shank2*$^{-/-}$ SC-CA1 synapses, and normal NMDA/AMPA ratio in the medial prefrontal cortex of *Shank2*$^{-/-}$ mice.

(a) Fast and slow decay time constants of NMDAR EPSCs were indistinguishable between WT and *Shank2*$^{-/-}$ SC-CA1 synapses (fast decay time constant, WT, 62.2 ± 12.5, KO, 80.4 ± 9.5; slow decay time constant, WT, 268.8 ± 34.1, KO, 311.5 ± 53.1; WT, 6 slices / 2 mice, KO, 6 slices / 2 mice, repeated measure two-way ANOVA, genotype effect, NS).

(b) *Shank2*$^{-/-}$ SC-CA1 synapses exhibited a comparable percentage of GluN2B-mediated EPSCs out of total NMDAR EPSCs, compared with WT mice. GluN2B-specific portion of NMDAR EPSCs were determined by using Ro 25-6981, an GluN2B-specific antagonist (WT, 35.6 ± 3.9, 6 slices / 2 mice; KO, 37.0 ± 5.2, 6 slices / 2 mice; Student's t-test, NS).

(c) Normal ratio of NMDAR- to AMPAR-mediated transmission (NMDA/AMPA ratio) in the prelimbic area of the medical prefrontal cortex in *Shank2*$^{-/-}$ mice. The NMDA/AMPA ratio was obtained by measuring AMPAR transmission at a holding potential of -70 mV, and NMDAR transmission at +40 mV with CNQX bath-application (WT, 0.80 ± 0.08, 9 slices / 3 mice; KO, 0.68 ± 0.08, 9 slices / 3 mice; NS, not significant, Student's t-test).

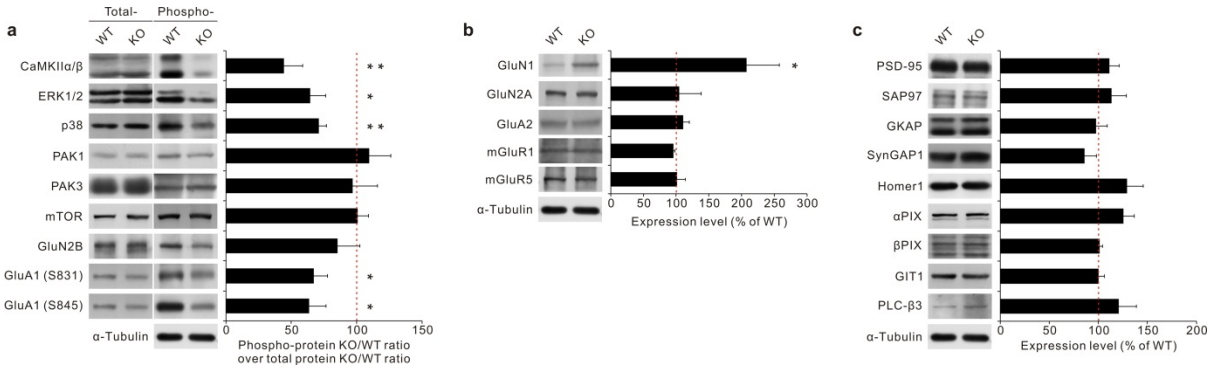

Supplementary Fig. 15. Reduced NMDAR-associated signaling in the *Shank2*$^{-/-}$ brain.

Whole brain homogenates from wild-type and *Shank2*$^{-/-}$ mice (3−4 wks) were immunoblotted for markers of NMDAR-associated signaling and their targets (a; total and phosphorylated; KO/WT ratios of phospho-proteins were normalized by KO/WT ratios of total proteins), glutamate receptors (b; GluNs/NMDARs, GluAs/AMPARs, and mGluRs; total proteins), and synaptic scaffolds and signaling adaptors/proteins directly or indirectly associated with Shank2 (c; PSD-95, SAP97, GKAP, SynGAP1, Homer1, α/βPIX, GIT1, and PLC-β3). All protein signals were normalized by α-tubulin before comparison between genotypes. n = 4 (WT), 4 (KO); *$P < 0.05$, **$P < 0.01$; Student's t-test.

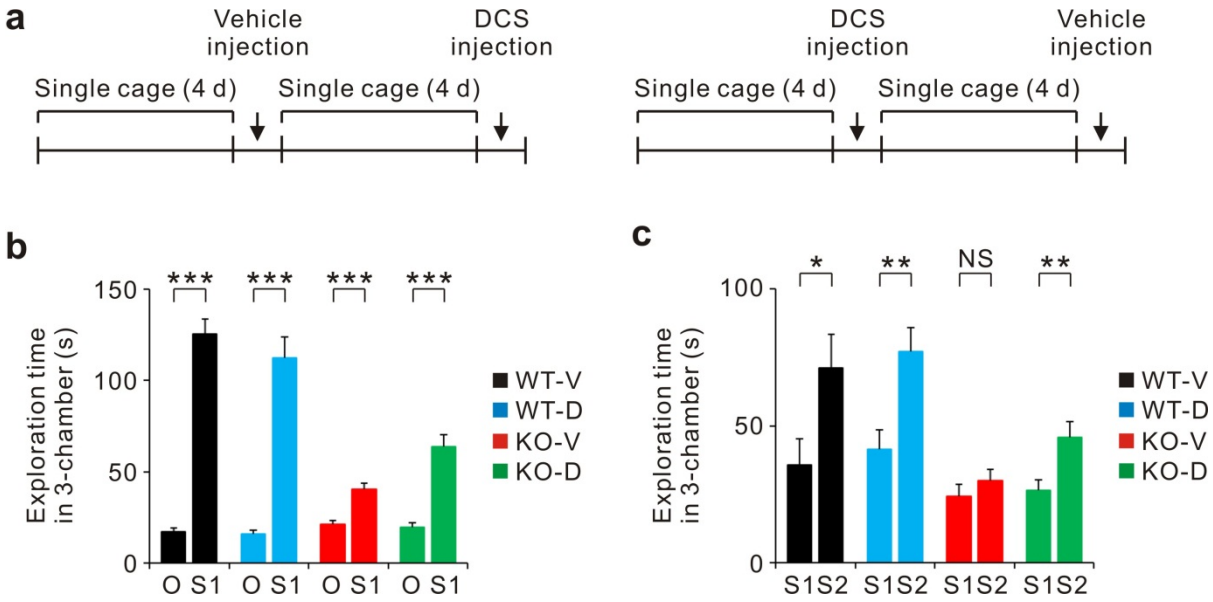

Supplementary Fig. 16. Drug treatment scheme and D-cycloserine-dependent improvement of social interaction of *Shank2*$^{-/-}$ mice in three-chamber assays.

(a) (Left) A group of *Shank2*$^{-/-}$ mice isolated in single cages for four days were treated with vehicle, followed by three-chamber assays, in which mice were allowed to explore an inanimate object (Object 1) or a novel mouse (Mouse 1). After this session and another four days of isolation, the same three mice were treated with D-cycloserine and subjected to the second round of three-chamber assays. Here we used a different object (Object 2) and a different novel mouse (Mouse 2) to minimize possible effects of remembering the Object 1/Stranger 1; Object 1 and Object 2 used here were proven to be equally preferred by *Shank2*$^{-/-}$ mice in the novel object recognition assays.

(Right) Another group of mice were D-cycloserine treated first and subsequently vehicle treated after four days, followed by three-chamber assays. Note that the same mice show different levels of mouse preference over inanimate objects upon vehicle/D-cycloserine treatment. We switched the order of vehicle/D-cycloserine treatment in the two groups (left and right) to reduce possibile influences of the first injection on the second experiment.

(b) D-cycloserine (20 mg kg^{-1}) partially normalizes the impaired three-chamber social interaction in *Shank2*$^{-/-}$ mice (KO-V/Vehicle and KO-D/D-cycloserine), as shown by exploration time, while it has no effect on wild-type mice (WT-V and WT-D).

(c) D-cycloserine (20 mg kg^{-1}) has no effect on recognition of social novelty both in *Shank2*$^{-/-}$ and wild-type mice, although an increasing tendency was observed by exploration time. n = 9 (WT-V), 10 (WT-D), 11 (KO-V), 10 (KO-D); *P < 0.05, **P < 0.01, ***P < 0.001, NS, not significant; Student's t-test.

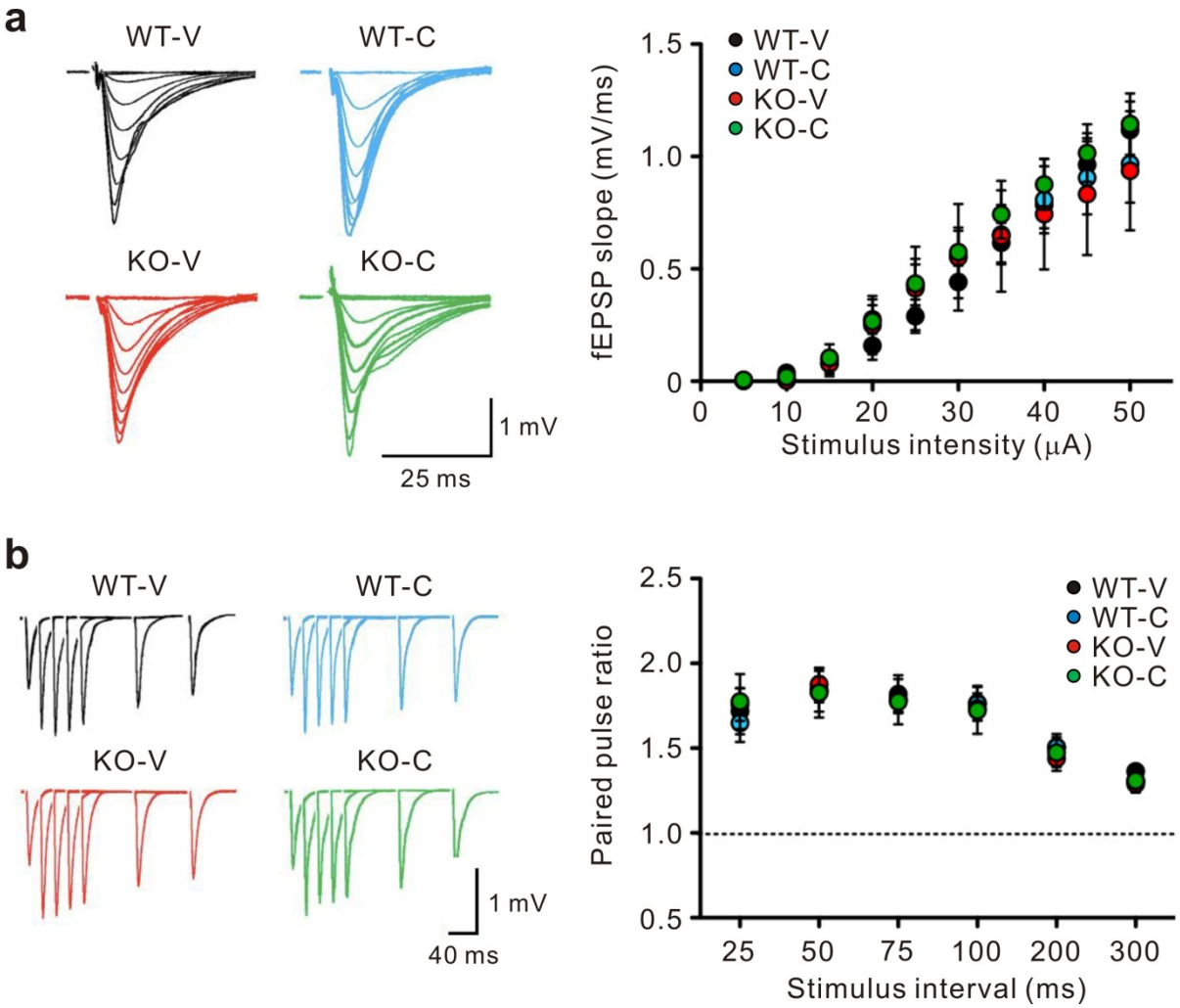

Supplementary Fig. 17. CDPPB has no effect on basal transmission and paired pulse ratio in *Shank2*$^{-/-}$ mice.

CDPPB treatment has no effect on basal transmission (a; input-output curve) and paired pulse ratio (b) in *Shank2*$^{-/-}$ mice (KO-C) or wild-type (WT-C) mice, relative to vehicle-treated *Shank2*$^{-/-}$ mice or wild-type mice (KO-V and WT-V). Acute slices were treated with CDPPB (10 μM) 20 min prior to and during the whole period of input-output and paired pulse ratio recordings at SC-CA1 synapses (basal transmission/input-output, WT-V, 8 slices / 4 mice, WT-C, 8 slices / 4 mice, KO-V, 8 slices / 5 mice, KO-C, 8 slices, 2 mice; paired pulse ratio, WT-V, 6 slices / 3 mice, WT-C, 8 slices / 4 mice, KO-V, 8 slices / 4 mice, KO-C, 5 slices, 2 mice).

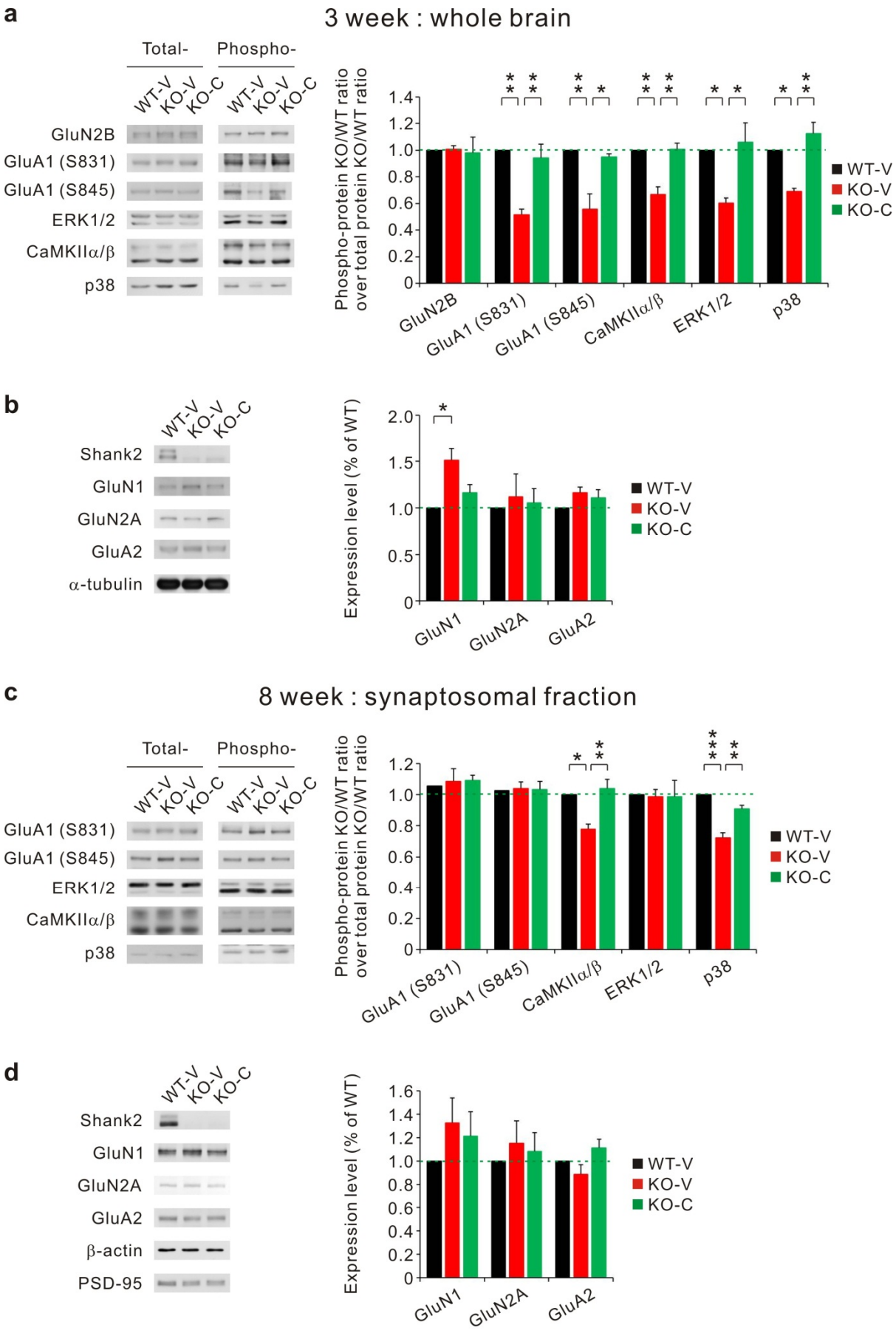
a
3 week : whole brain
Total-
Phospho-
WT-V
KO-V
KO-C
GluN2B
GluA1 (S831)
GluA1 (S845)
ERK1/2
CaMKIIα/β
p38
Phospho-protein KO/WT ratio over total protein KO/WT ratio
WT-V
KO-V
KO-C
b
Shank2
GluN1
GluN2A
GluA2
α-tubulin
Expression level (% of WT)
c
8 week : synaptosomal fraction
d
β-actin
PSD-95

Supplementary Fig. 18. CDPPB rapidly and fully normalizes NMDAR-associated signaling in the whole brain of 3-wk-old *Shank2*$^{-/-}$ mice and synaptosomes of 8-wk-old *Shank2*$^{-/-}$ mice.

(a–b) Whole brain samples from *Shank2*$^{-/-}$ mice (3 wks), treated with CDPPB (10 mg kg^{-1}; KO-C) 40 min prior to whole brain preparation, show recoveries in phosphorylation levels of the indicated proteins, as compared with vehicle-treated *Shank2*$^{-/-}$ mice (KO-V) and wild-type animals (WT-V) (a). In addition to phospho-proteins, total proteins were also compared (b), where the three groups showed no differences. n = 3 (WT-V), 3 (KO-V), 3 (KO-C); *P < 0.05, **P < 0.01; one-way ANOVA.

(c–d) Synaptosomal samples from *Shank2*$^{-/-}$ mice (8 wks), treated with CDPPB (10 mg kg^{-1}; KO-C) 40 min prior to synaptosome preparation, show recoveries in phospho-protein levels (c) such as CaMKIIα/β (lower/upper band) and p38, as compared with vehicle-treated *Shank2*$^{-/-}$ mice (KO-V) and wild-type animals (WT-V). In addition to phospho-proteins, total proteins were also compared (d), where the three groups showed no differences. n = 3 (WT-V), 3 (KO-V), 3 (KO-C); *P < 0.05, **P < 0.01, ***P < 0.001; one-way ANOVA.

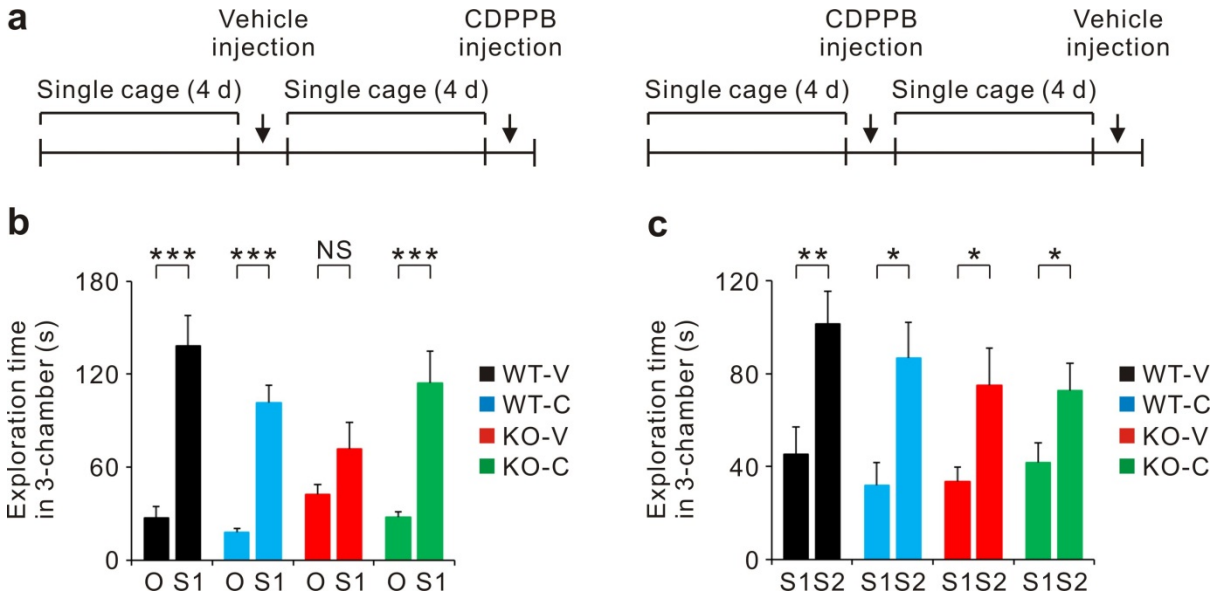

Supplementary Fig. 19. Drug treatment scheme and CDPPB-dependent improvement of social interaction of *Shank2*$^{-/-}$ mice in three-chamber assays.

(a) CDPPB treatment scheme.

(b and c) CBPPB improves social interaction in *Shank2*$^{-/-}$ mice, while it has no effect on the recognition of a novel mouse (Stranger 2) by by *Shank2*$^{-/-}$ mice, as indicated by time spent exploring the Stranger 1 (S1) vs. Object (O) (b), or Stranger 2 (S2) vs. Stranger 1 (S1) (c). n = 8 (WT-V/Vehicle), 8 (WT-C/CDPPB), 9 (KO-V), 9 (KO-C); *P < 0.05, **P < 0.01, ***P < 0.001, NS, not significant; Student's t-test.

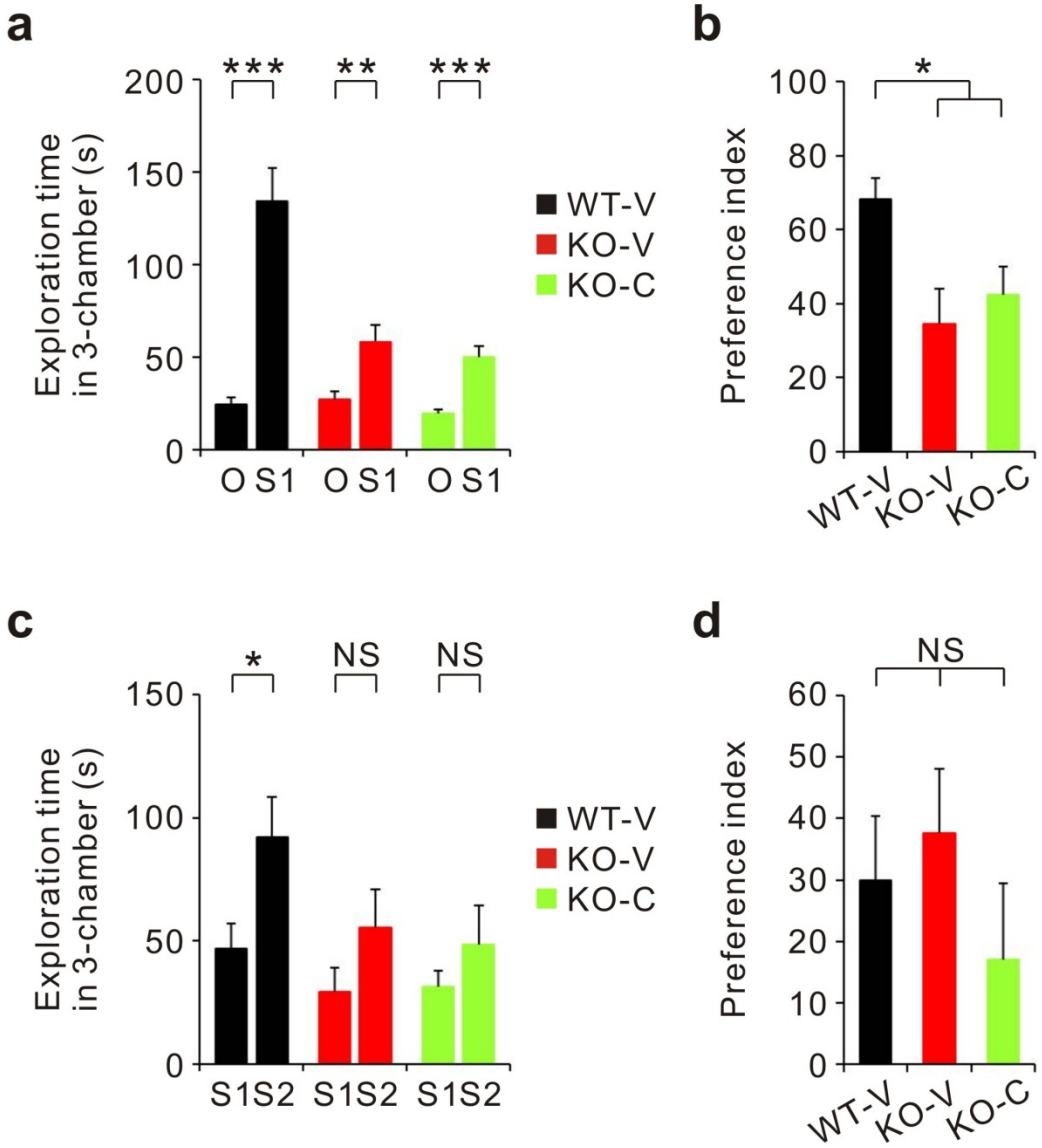

Supplementary Fig. 20. A lower-dose CDPPB does not rescue three-chamber social interaction in *Shank2*$^{-/-}$ mice.

Shank2$^{-/-}$ mice (2–5 months) treated with a lower-dose CDPPB (3 mg kg^{-1}; KO-C) do not show rescued social interaction, as shown by exploration time (a) and preference index (b), as compared with *Shank2*$^{-/-}$ mice treated with vehicle (KO-V) or wild-type mice treated with vehicle (WT-V). In addition, CDPPB (3 mg kg^{-1}) had no effect on recognition of social novelty in *Shank2*$^{-/-}$ mice (c and d). n = 10 (WT-V), 7 (KO-V), 7 (KO-C); *P < 0.05, **P < 0.01, ***P < 0.001, NS, not significant; Student's t-test (exploration time) and one-way ANOVA (preference index).

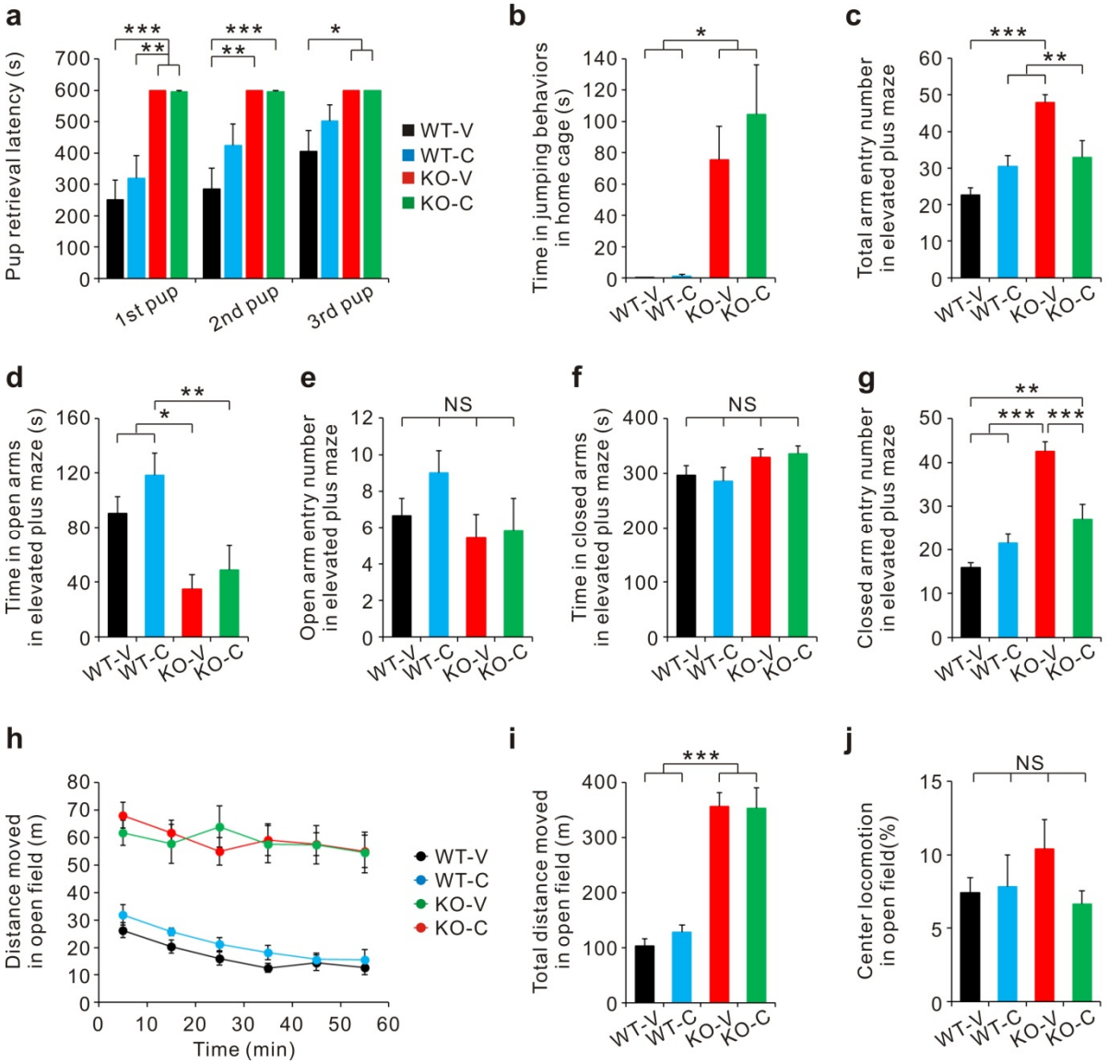

Supplementary Fig. 21. CDPPB does not rescue pup retrieval, repetitive jumping, anxiety-like behavior, and hyperactivity in *Shank2*$^{-/-}$ mice.

CDPPB (10 mg kg^{-1}) did not rescue impaired pup retrieval (a), repetitive jumping (b), anxiety-like behavior in an elevated plus-maze (c–g), or hyperactivity in an open field (h–j) in *Shank2*$^{-/-}$ mice (2–5 months). Note, however, that CDPPB rescues hyperactivity in the elevated plus-maze (c and g), although not in an open field (h and i), which is a standard assay for hyperactivity. Pup retrieval, n = 11 (WT-V/Vehicle), 7 (WT-C/CDPPB), 6 (KO-V), 11 (KO-C); repetitive behaviors, n = 7 (WT-V), 7 (WT-C), 7 (KO-V), 7 (KO-C); elevated plus maze, n = 9 (WT-V), 7 (WT-C), 7 (KO-V), 7 (KO-C); open field, n = 8 (WT-V), 8 (WT-C), 8 (KO-V), 8 (KO-C); *P < 0.05, **P < 0.01, ***P < 0.001, NS, not significant; One-way ANOVA (all others) and repeated measure of ANOVA for pup retrieval (a) and open field (h).

SUPPLEMENTARY METHODS

Generation of *Shank2*$^{-/-}$ mice. The targeting vector was designed to replace a ~3.1 kb genomic fragment of the *Shank2* gene with a positive selection marker (MC1 promoter and neomycin resistance gene). In addition, negative selection marker (HSV-1 promoter driven thymidine kinase gene) was appended to the construct to select against non-homologous recombination. To delete the exons 6 and 7 corresponding to the PDZ domain of *Shank2* (exon numbers were assigned by cDNA sequence of Shank2b [NM_001113373]), 5'- and 3'-flanking DNA sequences were isolated from the 129/SvJ mouse genomic DNA by PCR using two sets of oligonucleotide primers. A 7.3 kb *NotI-SalI* fragment derived from a 5' region of *Shank2* exon 6 was used as the left arm of the targeting vector: forward primer (*NotI*) 5'-AAG GAA AAA AGC GGC CGC ACC CAG GAA CTG GGA ACC AGT AAC TGC TGA GAT CCT AGA GGC CAG TGG ATG GCC ATG TGT G-3'; reverse primer (*SalI*) 5'-TTC CGC GGC CGC TAT GGC CGA CGT CGA CAT TTC AGT CCT ACC AGA GCC AAG GAG GGC AGC GGC TCC CT-3'. A 2.7 kb *XhoI-NheI* fragment derived from a 3' region of *Shank2* exon 7 was used as the right arm: forward primer (*XhoI*) 5'-CCG CTC GAG AAA GCA GGA TAA TGT TGG TCA TTT GAG GAG TCT TCT TGT GTG CAA GTG TTG GTG TCT GTG AAC GTC ACC TGC GGG TTG TAT GTT GGT GCC AGT GAG GAA-3'; reverse primer (*NheI*) 5'-CTA GCT AGC CCT AAG CGA TTT AGT CTA ACA GCC ATG GAC AAA GCC TTT ACT ATA TAG TGT AAG CAT GGA GTG CTG CTC TCA AGT CTC AA-3'. The 5'-long arm and 3'-short arm fragments were subcloned into the pOsdupdel plasmid. The targeting vector was linearized with *Not*I and electroporated into 129/SvJ mouse J1 embryonic stem cells. Clones resistant to G418 and gancyclovir were selected, and homologous recombination was confirmed by Southern blotting. The S*hank2* gene was modified in 6 of 210 clones screened. The three clones containing the targeted mutation were

injected into C57BL/6N blastocysts, and these were subsequently transferred into pseudopregnant foster mothers. The resulting male chimeric mice were bred to C57BL/6N females to obtain heterozygous *Shank2* (*Shank2*$^{+/-}$) mice. Germ-line transmission of the mutant allele was verified by Southern blot analysis of tail DNA from F1 offspring with agouti coat color. Interbreeding of the heterozygous mice was performed to generate homozygous *Shank2*-deficient (*Shank2*$^{-/-}$) mice. After initial confirmation of the deletion of *Shank2* gene in mice, *Shank2*$^{+/-}$ mice were established and maintained by backcrossing to C57BL/6 mice for more than five generations. The mice were bred and maintained according to the Yonsei Medical Center, KAIST, and Seoul National University Animal Research Requirements, and all procedures were approved by the Committees on Animal Research at Yonsei Medical Center (protocol number 09-127), KAIST (KA2010-18), and Seoul National University (SNU-110809-1). Mice were fed *ad libitum* and housed under 12-h light cycle. For behavioral experiments, we used hetero x hetero breeding and strict sex-matched controls.

Characterization of *Shank2*$^{-/-}$ mice. For Southern blot analysis, genomic DNAs obtained from J1 embryonic stem cells and mice were screened by a probe covering regions just outside to the 3'-short arm of the knockout vector. The 947-bp Southern probe was generated by PCR using oligonucleotide primers (5'-CAC AGA GTG CCA GGA ATT CTG-3' and 5'-TGG AGG GAG CAG TAG TAT TGG-3'). Wild-type and mutant alleles of mice were confirmed by two sets of genotyping oligonucleotide primers; wild-type, 5'-GCT AGC ATG ACG TGT GTT GTG-3', 5'-CCG ACT GCA TCT GCG TGT TC-3' (PCR product size: 525 bp); *Shank2*$^{-/-}$, 5'-CCA CTG CAT CTG CGT GTT C-3', 5'-CCG ACT GCA TCT GCG TGT TC-3' (PCR product size: 591 bp).

RNA extraction, cDNA synthesis, RT-PCR, and quantitative real-time PCR. Total RNA was extracted from the pancreas and brain tissues of wild-type and *Shank2*$^{-/-}$ mice. Purified RNA samples were reverse transcribed by using the iScript^{TM} Select cDNA Synthesis Kit (Bio-Rad, Hercules, CA) according to the manufacturer's instructions. The primers used in the RT-PCR analysis were primer 1 (Exon 6 Sense: GAC AAG ACG GTG GTC CTG), primer 2 (Exon 7 Sense TGC AGT ACC TGG AGT CCG), and primer 3 (Exon 12 Anti-Sense: GGA CCG TGG GCG TCA TTA). Exon numbers are based on Shank2b (NM_001113373). Reverse transcription for 60 min at 42 ℃ was followed by 30 PCR cycles. The PCR products were visualized by staining with ethidium bromide in a 2% agarose gel. Quantitative real-time PCR was performed by using the TaqMan Gene Expression Assay Kit (Applied Biosystems) according to the manufacturer's instructions. Briefly, 1 mL of cDNA was mixed with 10 mL of 2X TaqMan Universal Master Mix and 1 mL of the 20X TaqMan Gene Expression Assay, and was brought to a total volume of 20 mL with RNase-free water. Target amplification was performed in 96-well plates by using StepOnePlus^{TM} Real-Time PCR System (Applied Biosystems). TaqMan probes for *Shank2* (Mm01163746_mH and Mm01163737_m1) and glyceraldhyde-3-phosphate dehydrogenase (*Gapdh*) (Mm99999915_g1) were purchased from Applied Biosystems. Mm01163746_mH probe recognizes exons 3-4, whereas Mm01163737_m1 recognizes exons 15-16. PCR thermal cycling conditions included an initial 10 minutes at 95℃ to activate the AmpliTaq Gold DNA polymerase, followed by 40 cycles of denaturation (15 seconds at 95℃) and annealing/primer extension (15 seconds at 60℃). All samples were performed in triplicate. The relative RNA expression levels were calculated via a comparative threshold cycle (C_t) method using *Gapdh* as control: $\Delta Ct = Ct(Gapdh) - C_t(Shank2)$. The gene expression fold change, normalized to the *Gapdh* and relative to the control sample, was calculated as $2^{-\Delta\Delta Ct}$.

Social interaction assay in home cages. Stranger mice (2–4 months old) were placed in a transparent plastic apparatus (15 × 8 × 12 cm). In the beginning, the empty apparatus without a stranger mouse was placed in the home cage of a test mouse (wild-type or *Shank2*$^{-/-}$ mouse). After 10 minutes of free exploration of the container by the test mouse, a stranger mouse was placed in the apparatus, and the test mouse was allowed to explore the stranger mouse for 10 min. Exploration was defined as each instance in which wild-type or *Shank2*$^{-/-}$ mouse tries to sniff the stranger mouse, or orients its nose towards and come close to the stranger. Experiments and analyses were performed by independent researchers in a blind manner.

Three-chamber social interaction assay. The three-chamber social interaction assay consisted of three phases. In the first phase, a wild-type or *Shank2*$^{-/-}$ mouse was placed in the three-chambered apparatus with two small containers in the left or right (not center) chamber, and was allowed to explore the environment freely for 10 min for habituation. After 10 min, the wild-type or *Shank2*$^{-/-}$ mouse was gently guided to the center chamber, and the two entrances to the center chamber were blocked while an inanimate object (Object) and a stranger mouse (Stranger 1) were placed in the two containers. Then, the two entrances were opened to allow the mouse in the center to explore the new environment freely for 10 min. In the third phase, the test mouse was gently guided to the center chamber again, with the blockade of the entrances. The Object was replaced with Stranger 2, followed by exploration of the Stranger 1 or 2 by the test mouse for 10 min. Exploration was defined as each instance in which wild-type or *Shank2*$^{-/-}$ mouse tries to sniff Object/Stranger, or orients its nose towards and come close to Object/Stranger. Time spent in each chamber was measured by Ethovision 3.1 program (Noldus). Individual movement tracks were analyzed by Ethovision and modified by ImageJ to generate heat maps. In addition to time spent in chamber or exploration, we used the preference index, which represents a numerical difference between

times spent exploring the targets (Stranger1 vs. Object, or Stranger 2 vs. Stranger 1) divided by total time spent exploring both targets, as described previously [1].

Olfactory function test. This experiment was performed as described previously [2]. A piece of Kim-wipes was soaked with 20 μl of water or non-social cues (banana and coffee). To generate social cues, several Kim-wipes were introduced to a stranger mouse's cage for 2 days before the experiment. The wipers were retrieved from the stranger mouse's cage right before the experiment, and used for social cues. These non-social and social cues were contained in small round shaped petri dishes with holes. WT or *Shank2*$^{-/-}$ mice were introduced to mock for 30 min before the experiment. Water, non-social cues, and social cues were introduced sequentially to the homecages of WT or *Shank2*$^{-/-}$ mice for 6 min each. Cues were retrieved from the homecage after each session, and inter-session interval was 1 min. The sniffing behavior toward cue-containing petri dishes was measured in a blind manner.

Morris water maze assay. Mice were trained to find the hidden platform (10 cm diameter) in a 120 cm diameter white plastic tank. Mice were given 3 trials per day with an inter-trial interval of 1 hr. Training was performed for six consecutive days, and the probe test was given for 1 min with the platform removed from the pool at day 7 (24 h after the last training session). Percentage of time spent in four quadrants of the pool (T, target; O, opposite; L, left; R, right), the number of exact crossings over the platform area, and swimming speed were evaluated by Ethovision 3.1 program (Noldus).

Novel object recognition assay. Object recognition test was performed in an open field apparatus. During the sample phase, mice were allowed to explore two identical objects for

10 min. Test phase, where one of the two objects was replaced with a new one, was performed 24 h later, and exploration time for the two objects was measured. Object exploration was defined as each instance in which a mouse's nose touched the object or was oriented toward the object and came within 2 cm of it.

Ultrasonic vocalization (USV). To induce courtship USVs in male mice, a female was introduced into the male resident cage. USV recordings were made with 12-week-old male mice. Each male was isolated in a transparent acrylic housing cage for at least three days before the recording of their courtship USVs. On the recording day, mice were placed in the recording chamber for 30 min. After a 5 min background recording, one randomly chosen estrus B6 female (3–5 months old, 4–5 mice housed together) was placed in the recording chamber. The estrus stage was confirmed in female mice. A male was allowed to investigate the female for 5 min, and emitted USVs were recorded. USVs were recorded through a quarter-inch microphone and amplified with a preamplifier and a main amplifier (sound recording from Brüel and Kjaer Inc., Denmark). Signals were filtered from 1 Hz to 100 kHz and digitized with a sampling frequency of 250 kHz, 16 bits per sample, using a 1000 Hz high-pass digital filter (model 1322A, Axon Instruments, Union City, CA). Sound recordings were processed using a custom Matlab program. Short-time Fourier transform analysis was performed to draw sonograms (1,024 samples/block, 1/4 overlap, resulting in a time resolution of 1.02 ms and a frequency resolution of 0.45 kHz). Frequencies lower than 35 kHz were filtered out to reduce background white noise and audible squeaking from females. As a basal power spectrum, consecutive powers of 10 s without USVs were sampled and averaged for time, such that 1.2 times the basal power spectrum was subtracted from each power spectrum and frequencies with a power less than zero were set to zero. This procedure was used to reduce the background white noise.

Pup retrieval assay. Virgin female mice were isolated for four days before pup retrieval assays. Three normal pups (1-d old; C57BL/6N) were placed at three different corners of a home cage of a test female mouse (wild-type or *Shank2*$^{-/-}$), and the female mouse was allowed to retrieve the pups for 10 min. Efficiency of pup retrieval was measured by the time taken to retrieve the first, second, and third pups.

Repetitive behaviors. Mice in their home cages with fresh bedding were used to measure times spent in repetitive behaviors including jumping, upright scrabbling, grooming, and digging during 10 min. Jumping was defined as the behavior of a mouse where it rears on it hind legs at the corner of the cage, or along the side walls, and jumps so that the two hind legs are simultaneously off the ground. Upright scrabbling was defined as the behavior of a mouse where it rears on it hind legs at the corner of the cage, or along the side walls, and tries to climb up against the wall with the two hind legs alternatively or coordinately touching the ground. Grooming behavior was defined as stroking or scratching of face, head, or body with the two forelimbs, or licking body parts. Digging behavior was defined as the behavior of a mouse where it coordinately uses two fore legs or hind legs to dig out or displace bedding materials. Because *Shank2*$^{-/-}$ mice showed jumping behaviors significantly mixed with upright scrabbling behaviors, we could not separate the two behaviors, and labeled this behavior as jumping with the explanation in the text and figure legend.

Nest building assay. The isolated test mice were given a folded Kimwipes tissue as a nest-building material a day before the measurements of nesting behavior. The status of nesting material was photographed each day for 3 days. Nesting was scored based on the extent of conversion of the nesting material into fine pieces.

Open field assay. The size of the open field box was 40×40×40 cm, and the center zone line was 10 cm apart from the edge. Mice were placed in the center of chamber in the beginning of assay, and mouse movements were recorded with a video camera for 60 min, and analyzed by Ethovision 3.1 program (Noldus).

Elevated plus-maze. The elevated plus-maze consisted of two open arms, two closed arms, and a center area, elevated to a height of 50 cm above the floor. Mice were placed in the center area and allowed to explore the space for 8 min.

Light-dark test. The apparatus for light-dark test consisted of light (~600 lx) and dark (~5 lx) chambers adhered to each other. An entrance enabled mice to freely move across the light and dark chambers. The size of light chamber was 20 x 30 x 20 cm, and that of dark chamber was 20 x 13 x 20 cm. Mice were introduced to the center of light chamber with their heads pointing towards the opposite side of the dark chamber, and allowed to explore the apparatus freely for 10 min. The latency to enter the dark chamber, the time spent in dark and light chambers, and the number of transitions were measured. Transition was defined as the translocation of all four feet of mice from one to another chamber.

Electron microscopy. Wild-type and *Shank2*$^{-/-}$ mice (8–9 wks) were deeply anesthetized with sodium pentobarbital (80 mg kg^{-1}, i.p.) and were intracardially perfused with 100 ml of heparinized normal saline, followed by 500 ml of a freshly prepared fixative of 2.5% glutaraldehyde and 1% paraformaldehyde in 0.1 M phosphate buffer, pH 7.4. Hippocampus was removed from the whole brain and sectioned with a Vibratome at 100 μm thickness. The sections were postfixed in the same fixative for 2 h, osmicated with 1% osmium tetroxide in 0.1 M phosphate buffer for 1 h, dehydrated in graded alcohols, flat embedded in Durcupan

ACM (Fluka), and cured for 48 h at 60°C. Small pieces containing CA1 stratum radiatum (~150 μm from CA1 pyramidal cell body layer) were cut out of the wafers and glued onto the plastic block by cyanoacrylate. Ultrathin sections were cut and mounted on Formvar-coated single slot grids, stained with uranyl acetate and lead citrate, and examined with an electron microscope (Hitachi H-7500; Hitachi) at 80 kV accelerating voltage. Randomly selected neuropil areas within 120–150 μm from cell body were photomicrographed at a 40,000× and used for quantification. Thirty electron micrographs representing 435.5 μm^2 neuropil regions in each mouse were taken. Number of spines (PSD density), proportion of perforated spines, PSD length and PSD thickness from three wild-type and *Shank2*$^{-/-}$ mice were quantified. The measurements were all performed by an experimenter blind to the genotype. Digital images were captured with GATAN DigitalMicrograph software driving a CCD camera (SC1000 Orius; Gatan) and saved as TIFF files. Brightness and contrast of the images were adjusted in Adobe Photoshop 7.0 (Adobe Systems).

Electrophysiology. All the recordings were done as described previously [4]. For extracellular recordings, transverse hippocampal slices (400 μm) were prepared from WT and *Shank2*$^{-/-}$ mice and slices were maintained in an interface chamber at 28 °C. The artificial cerebrospinal fluid (ACSF) contained 124 mM NaCl, 2.5 mM KCl, 1 mM NaH_2PO_4, 25 mM $NaHCO_3$, 10 mM glucose, 2 mM $CaCl_2$, and 2 mM $MgSO_4$, and oxygenated with 95 % O_2 and 5 % CO_2. Extracellular field EPSPs (fEPSPs) were recorded in stratum radiatum of CA1 using a glass pipette filled with ACSF (1 MΩ). The SC pathway was stimulated every 30 s using bipolar electrodes (MCE-100; Kopf Instruments). fEPSPs were amplified (GeneClamp 500; Molecular Devices), and digitized (PCI-6221; National Instruments) for measurement. Data were monitored, analyzed using the WinLTP program (http://www.ltp-program.com). For LTP and LTD, the stimulation intensity was adjusted to give fEPSP slopes of 40 % of

maximum and two successive responses were averaged and expressed relative to the normalized baseline. After a stable baseline was recorded, high frequency stimulation (HFS)-LTP (100 Hz, 1 s), theta-burst stimulation (TBS)-LTP (10 trains of 4 pulses at 100 Hz, delivered at an inter-train interval of 200 ms, repeated 4 times at 10 s interval), and low frequency stimulation (LFS)-LTD (1 Hz, 900 pulses) were induced. In mGluR LTD, DHPG (100 μM) was bath-applied for 15 min after baseline recording.

For NMDA/AMPA ratio experiments, coronal hippocampal or mPFC (prelimbic cortex) slices (300 μm) were prepared from WT and *Shank2*$^{-/-}$ mice. The recording pipettes (3~5 MΩ) were filled with an internal solution containing 100 mM CsOH, 100 mM D-gluconate, 10 mM EGTA, 10 mM HEPES, 5 mM NaCl, 20 mM TEA-Cl, 4 mM MgATP, 0.3 mM Na3GTP, 3 mM QX-314 (280~300 mOsm, pH 7.2 with CsOH). Pyramidal neurons in CA1 were voltage-clamped at -70 mV, and EPSCs were evoked at 0.05 Hz. AMPA receptor-mediated EPSCs were recorded at -70 mV, and 30 consecutive responses were recorded after stable baseline. After recording AMPA-mediated EPSCs, CNQX (20 μM) were applied to ACSF and holding potential was changed to +40 mV to record NMDA receptor-mediated EPSCs. The NMDA/AMPA ratio was calculated by dividing the mean value of 30 NMDA receptor-mediated EPSC peak amplitudes by the mean value of 30 AMPA receptor-mediated EPSC peak amplitudes. For NMDA/AMPA ratio in mPFC, layer II/III in prelimbic cortex was stimulated and whole-cell recording was conducted in layer V pyramidal neurons. Picrotoxin (100 μM) was always present to block GABAA receptor-mediated currents. Access resistance was 15~25 MΩ, and only cells with a change in access resistance < 20 % were included in the analysis

For mEPSC measurements, tetrodotoxin (1 μM) was included in the ACSF and the amplitude and frequency of mEPSCs were analyzed with MiniAnalysis program

(Synaptosoft). For measurement of neuronal excitability, an internal solution containing 145 mM K-gluconate, 5 mM NaCl, 10 mM HEPES, 2 mM MgATP, 0.1 mM Na_3GTP, 0.2 mM EGTA, and 1 mM $MgCl_2$ (280~300 mOsm, pH 7.2 with KOH) was used and action potentials were elicited by applying depolarization current pulses under current clamp configuration. For the analysis of NMDAR-mediated EPSC decay, NMDAR-mediated EPSC was first isolated at +40 mV holding potential in the presence of CNQX (20 μM) and the decay phase of NMDAR EPSC was fitted with a double exponential function (Clampex 9.2; Molecular Devices). For GluN2B-mediated EPSC, NMDAR EPSC was first monitored at +40 mV and after stable baseline, Ro 25-6981 (5 μM) was applied to isolate GluN2B -mediated component of NMDAR EPSC.

CDPPB (10 μM) or D-cycloserine (20 μM) was bath-applied for 20 and 35 min prior to LTP and LTD induction, respectively, or from 20 min prior to and during the whole period of NMDA/AMPA ratio recording. Whole-cell patch recordings were performed using Axopatch 200B (Molecular Devices), and monitored and analyzed using Clampex 9.2 (Molecular Devices). Drugs were purchased from Ascent Scientific (CDPPB and D-cycloserine), Tocris (DHPG, CNQX, Ro 25-6981, tetrodotoxin), and Sigma (picrotoxin).

Antibodies. GIT1 (Du139) and PLC-β3 antibodies were kind gifts from Drs. Premont and Suh, respectively. Antibodies against PSD-95 (#1402), Homer1 (#1133), and CaMKII (#1298) were generated in our laboratory. The following antibodies have been described: Shank2 (#1136) [5], βPIX (#1254) [6], GKAP (#1243) [7], SynGAP1 (#1682) [8], GluA1/GluR1 (#1193) [8], and GluA2/GluR2 (#1195) [7], SAP97 (#1443) [9]. The following antibodies were purchased: GIT1 and Shank2 N-term (NeuroMab); αPIX, phospho-PAK1/3 (Thr 423), ERK1/2, phospho-ERK1/2 (Thr 202, Tyr 204), mTOR, phospho-mTOR (Ser 2448), p38, and phospho-p38 (Thr 180, Tyr 182) (Cell Signaling); PAK1, PAK3, (Santa Cruz); GluN1/NR1, vGlut1,

vGAT (SySy); glutamate, α-tubulin, β-actin (Sigma); GluN2A/NR2A (Invitrogen); GluN2B/NR2B (BD Transduction Laboratories); phospho-CaMKIIα/β (Thr 286), GABA (Abcam); NeuN, GAD67, phospho-GluA1 (Ser 831), phospho-GluA1 (Ser 845), phospho-GluN2B (Ser 1303), mGluR1, mGluR5 (Millipore).

Preparation of whole brain homogenates and synaptosomes. For whole brain homogenates, mouse brains (3–4 wks) were briefly homogenized in 3 volumes of ice-cold homogenization buffer (0.32 M sucrose, 10 mM HEPES pH7.4, 2 mM EDTA, protease inhibitors, phosphatase inhibitors). Protein concentrations were measured by the Bradford assay. The relative amount of α-tubulin was used as a loading control. Synaptosomal fractions were prepared as previously described [10].

Immunohistochemistry. Brains were isolated from adult mice (3 months old) after cardiac perfusion (4% paraformaldehyde). After the post-fixation for 12 h, 50 μm brain sections were obtained by vibratome. Brain sections were washed 3 times with phosphate-buffered saline for 10 min, permeabilized with 0.5% TritonX-100 for 30 min, blocked with 5% bovine serum albumin (BSA) for 1 h, stained with primary antibodies at 4 °C for 12 h, stained with secondary antibodies for 1 h, and mounted with Vectashield (Vector). For quantitative analysis, images of brain sections were captured with a confocal microscope (×5 and ×63 objectives; Leica Microsystems) and analyzed using Metamorph (Molecular Devices).

Pharmacological rescue. CDPPB (Ascent scientific) was dissolved in DMSO and polyethylene glycol 400 (DMSO:PEG 400 = 1:9) to a final concentration of 6 g l^{-1}. Wild-type and *Shank2*$^{-/-}$ mice received intraperitoneal injection of CDPPB (10 or 3 mg kg^{-1}), or the same volume of DSMO-PEG400 mixture, 30 min before three-chamber or other behavioral

assays and 40 min before brain sample preparation for immunoblot analyses. D-cycloserine (Ascent Scientific) was dissolved in saline to final concentration of 12 g l^{-1}. Wild-type and *Shank2*$^{-/-}$ mice received intraperitoneal injection of D-cycloserine (20 mg kg^{-1}), or the same volume of saline, 30 min before three-chamber assays.

References for Methods

1. Wang, X. et al. Synaptic dysfunction and abnormal behaviors in mice lacking major isoforms of Shank3. Hum Mol Genet 20, 3093-108 (2011).
2. Yang, M. & Crawley, J.N. Simple behavioral assessment of mouse olfaction. Curr Protoc Neurosci Chapter 8, Unit 8 24 (2009).
3. Kim, J.I. et al. PI3Kγ is required for NMDAR-dependent long-term depression and behavioral flexibility. *Nat Neurosci* (2011).
4. Ryan, B.C. et al. Social deficits, stereotypy and early emergence of repetitive behavior in the C58/J inbred mouse strain. Behav Brain Res 208, 178-8 (2010).
5. Han, W. et al. Shank2 associates with and regulates Na^+/H^+ exchanger 3. *J Biol Chem* 281, 1461-9 (2006).
6. Park, E. et al. The Shank family of postsynaptic density proteins interacts with and promotes synaptic accumulation of the beta PIX guanine nucleotide exchange factor for Rac1 and Cdc42. *J Biol Chem* 278, 19220-9 (2003).
7. Ko, J., Na, M., Kim, S., Lee, J.R. & Kim, E. Interaction of the ERC family of RIM-binding proteins with the liprin-alpha family of multidomain proteins. *J Biol Chem* 278, 42377-85 (2003).
8. Kim, M.H. et al. Enhanced NMDA receptor-mediated synaptic transmission, enhanced long-term potentiation, and impaired learning and memory in mice lacking IRSp53. *J Neurosci* 29, 1586-95 (2009).

9. Han, S. et al. Regulation of dendritic spines, spatial memory, and embryonic development by the TANC family of PSD-95-interacting proteins. *J Neurosci* 30, 15102-12 (2010).

10. Blackstone, C.D. et al. Biochemical characterization and localization of a non-N-methyl-D-aspartate glutamate receptor in rat brain. *J Neurochem* 58, 1118-26 (1992).

SUPPLEMENTARY TABLES

See separate Excel files (**Supplementary Tables 1 and 2**).

SUPPLEMENTARY MOVIE LEGENDS

Supplementary movie 1. A pup retrieval assay with a wild-type mouse.

Supplementary movie 2. A pup retrieval assay with a *Shank2*$^{-/-}$ mouse.

Supplementary movie 3. An example of repetitive jumping mixed with upright scrabbling in a *Shank2*$^{-/-}$ mouse.

Supplementary movie 4. An example of repetitive grooming in a *Shank2*$^{-/-}$ mouse.

Supplementary movie 5. An example of repetitive digging in a *Shank2*$^{-/-}$ mouse.